

1 Evaluation of MSL Curiosity rover SAM methane detections with the  
2 Mars Regional Atmospheric Modeling System (MRAMS)

3 Jorge Pla-Garcia<sup>1,2,3</sup>

4  
5 <sup>1</sup>Centro de Astrobiología (CSIC-INTA)  
6 28850 Torrejón de Ardoz, Spain

7  
8 <sup>2</sup>Space Science Institute  
9 4750 Walnut St, Suite 205  
10 Boulder, CO 80301

11  
12 <sup>3</sup>Southwest Research Institute  
13 1050 Walnut Street  
14 Boulder, CO 80302

15  
16 Corresponding Author:

17 Jorge Pla-García  
18 [jpla@cab.inta-csic.es](mailto:jpla@cab.inta-csic.es)

30	<b>Contents</b>	
31	<b>1. Introduction</b>	<b>4</b>
32	1.1 Review of ground-based and orbiter methane measurements	4
33	1.2 SAM methane detections at Gale crater	12
34	1.3 Previous modeling works of methane transport	16
35	<b>2 Mars methane modeling experiments</b>	<b>19</b>
36	2.1 Mars Regional Atmospheric Modeling System (MRAMS)	19
37	2.2 Martian clathrates subsurface model	22
38	2.3 MRAMS methane experiment scenarios	26
39	2.3.1 Punctual methane release scenarios	27
40	2.3.2 Steady state methane release scenarios	29
41	<b>3 Results</b>	<b>30</b>
42	3.1 Punctual methane release results	31
43	3.2 Steady State methane release results	35
44	<b>4 Discussion</b>	<b>40</b>
45	4.1 A possible explanation to the methane background seasonal cycle	44
46	4.2 Impact of the thermal inertia into the methane spikes	47
47	<b>5 Conclusion</b>	<b>49</b>
48	<b>6 Acknowledgements</b>	<b>53</b>
49	<b>7 Supplementary material</b>	<b>54</b>
50	<b>8 References</b>	<b>54</b>
51		

52 **Abstract**

53 The in situ detection of methane at Gale crater by the Tunable Laser Spectrometer  
54 (TLS) of the Sample Analysis at Mars (SAM) instrument suite aboard the MSL  
55 Curiosity rover has garnered significant attention because of the implications for the  
56 potential of indigenous Martian organisms (Webster et al. 2013, 2015). In the absence  
57 of a yet-to-be-confirmed rapid destruction mechanism, the photochemical lifetime of  
58 methane is on the order of several centuries. This is much longer than the atmospheric  
59 mixing time scale, and thus the gas should tend to be well mixed except when near a  
60 source or shortly after an episodic release. The observed spike of 7.2 parts per billion by

61 volume (ppbv) from the background of <1 ppbv, and then the return to the putative  
62 background level in 47 sols is, therefore, curious. The Mars Regional Atmospheric  
63 Modeling System (MRAMS) was used to study the transport and mixing of methane  
64 from specified source locations using tracers, and to investigate whether methane  
65 releases inside or outside of Gale crater are consistent with SAM observations. The  
66 model simulations indicate that there must be a steady state release to counteract  
67 atmospheric mixing, because the timescale of mixing in the crater is ~1 sol. The model  
68 also indicates that the timing of SAM sample ingestion is very important, because  
69 modeled methane abundance varies by one order of magnitude over a diurnal cycle with  
70 a steady state emission. It is difficult to reconcile the SAM peak methane detections  
71 with the atmospheric transport and mixing predicted by MRAMS **in the same periods**.  
72 The only plausible scenario is an intermittent local steady state release close to the rover  
73 with the additional restrictions that such releases must be globally rare or there must be  
74 an unknown rapid methane destruction mechanism.

75

## 76 **Highlights**

- 77 • MRAMS is used to study the transport and mixing of methane emissions in and  
78 around Gale Crater.
- 79 • Crater mixing timescales are ~1 sol during all seasons, much faster than  
80 previously estimated.
- 81 • Predicted methane abundances of a steady state source vary by an order of  
82 magnitude over a diurnal cycle.
- 83 • The local time of sample ingest may strongly impact methane abundance  
84 measurements.

- 85 • It is difficult to reconcile the SAM measurements with the transport and mixing  
86 predicted by MRAMS in the same periods. The only plausible scenario is an  
87 intermittent local steady state release close to the rover.
- 88 • Ground temperature may control the release of methane trapped in clathrates on  
89 seasonal timescales, implying a seasonal hemispheric difference in methane  
90 background levels.
- 91 • During summertime, those levels inside crater should be poorly correlated with  
92 ground temperature due to an inundation of methane poor external crater air  
93 from the northern winter hemisphere.

## 94 **1. Introduction**

### 95 **1.1 Review of ground-based and orbiter methane measurements**

96 The possibility of detecting methane in the Mars atmosphere has attracted a great  
97 deal of attention because methane is primarily (90-95%) produced by biological activity  
98 on Earth. The first reported detection of methane in the atmosphere of Mars was made  
99 with the Mariner 7 spacecraft Infrared Spectrometer (IRS), and was announced at press  
100 conference two days after the Mars flyby (Sullivan 1969); however, shortly after it was  
101 shown that the observed spectral signatures were actually from CO<sub>2</sub> ice. This event  
102 serves as a lesson on how difficult it is to identify from Earth or from Martian orbit the  
103 spectral lines of methane, how difficult is to interpret remotely sensed spectra with  
104 weak absorption features, and how important it is not to let preconceived ideas and  
105 desires undermine a subjective analysis (Pla-Garcia 2017). As Carl Sagan quoted,  
106 extraordinary claims require extraordinary evidence.

107        Despite the Mariner 7 incident, the search for methane on Mars has continued. Over  
108 the last 14 years, there have been several reports of methane detection from Earth and  
109 from Mars orbit, although the detections are controversial and not universally accepted.  
110 All the putative detections suffer from one or more problems: weak signal, poor spectral  
111 resolution, telluric line contamination, and instrument noise or performance issues.

112        As can be seen in the Table 1, different detections of methane in the Mars  
113 atmosphere have been reported since 1999 until today. The earliest report of martian  
114 atmospheric methane suggested a global average value of  $10\pm 3$  parts per billion by  
115 volume (ppbv) using the Fourier Transform Spectrometer at the Canada–France–Hawaii  
116 Telescope (capturing only a portion of the Martian disk) and searching for methane in  
117 the  $3.3\ \mu\text{m}$  spectral band (Krasnopolsky et al. 2004).

Type	Instrument	Observation	Mars Ls	Max. Value in ppbv (region)	Global avg (ppbv)	Reference
Earth based	FTS-CFHT	1999	88	-	10±3	Krasnopolsky et al. 2004
Martian orbit	TES-MGS	1999	180	~68 (Tharsis), ~64 (AT), ~60 (Elysium)	33±9	Fonti and Marzo 2010
Martian orbit	TES-MGS	1999	270	~26 (Tharsis), ~30 (AT), ~24 (Elysium)	6±2	Fonti and Marzo 2010
Martian orbit	TES-MGS	2000	0	~34 (Tharsis), ~32 (AT), ~32 (Elysium)	17±5	Fonti and Marzo 2010
Martian orbit	TES-MGS	2000	90	~30 (Tharsis), ~40 (AT), ~38 (Elysium)	14±4	Fonti and Marzo 2010
Martian orbit	TES-MGS	2001	180	~56 (Tharsis), ~62 (AT), ~60 (Elysium)	18±7	Fonti and Marzo 2010
Martian orbit	TES-MGS	2001	270	~24 (Tharsis), ~24 (AT), ~22 (Elysium)	5±2	Fonti and Marzo 2010
Martian orbit	TES-MGS	2002	0	~32 (Tharsis), ~28 (AT), ~30 (Elysium)	10±4	Fonti and Marzo 2010
Earth based	CSHELL-IRTF, NIRSPEC-Keck2	2003	155	<45 (TS, NF and SM)	6	Murina et al. 2009
Martian orbit	TES-MGS	2003	180	~58 (Tharsis), ~56 (AT), ~52 (Elysium)	30±8	Fonti and Marzo 2010
Martian orbit	TES-MGS	2003	270	~22 (Tharsis), ~20 (AT), ~20 (Elysium)	5±1	Fonti and Marzo 2010
Martian orbit	TES-MGS	2004	0	~30 (Tharsis), ~30 (AT), ~30 (Elysium)	9±3	Fonti and Marzo 2010
Martian orbit	TES-MGS	2004	90	~56 (Tharsis), ~60 (AT), ~40 (Elysium)	28±8	Fonti and Marzo 2010
Martian orbit	PFS-MEX	2004	330-350	-	10±5	Formisano et al. 2004
Martian orbit	PFS-MEX	2004	330-10	20±10 (Elysium)	-	Encrenaz 2008
Earth based	CSHELL-IRTF	2006	10	-	<14	Krasnopolsky et al. 2007
Earth based	CSHELL-IRTF	2006	10	<10 (VM, 63-93°W and 0 to 7°N); 3 outside this region	-	Krasnopolsky et al. 2012
Earth based	CSHELL-IRTF and NIRSPEC-Keck2	2006	17	4	3	Murina et al. 2009
Earth based	CRILES-VLT, CSHELL-IRTF, NIRSPEC-Keck2	2006	352	-	<7.8	Villanueva et al. 2013
Martian orbit	PFS-MEX	2004-2008	50	21 (-40E and +70E lon)	14±5	Geminale et al. 2008
Martian orbit	PFS-MEX	2004-2008	160-180	<45 (north polar region)	14±5	Geminale et al. 2011
Martian orbit	PFS-MEX	2004-2008	325	5 (-40E and +70E lon)	14±5	Geminale et al. 2008
Earth based	CRILES-VLT, CSHELL-IRTF, NIRSPEC-Keck2	2009	12	-	<6.6	Villanueva et al. 2013
Earth based	CSHELL-IRTF	2009	20	<8 (0-30°W)	-	Krasnopolsky et al. 2012
Earth based	CSHELL-IRTF	2010	70	<8 (30°W to 90°E and along the central meridian)	-	Krasnopolsky et al. 2011
Earth based	CRILES-VLT, CSHELL-IRTF, NIRSPEC-Keck2	2010	83	-	<7.2	Villanueva et al. 2013
In-situ (Mars sfc)	SAM-MSL	2013-2014	336-82	7.2 ± 2.1 (Gale crater)	-	Webster et al. 2015
Earth (~12-14 km)	SOFIA-EXES	2016	123	1 ± 5 ppb (several locations)	-	Aiko et al. 2017

Table 1. Detections of methane in the Mars atmosphere reported since 1999 until today

119 In the second detection, from Mars orbit observation, Formisano et al. 2004 used the  
120 Planetary Fourier Spectrometer (PFS) on board ESA Mars Express (MeX) spacecraft  
121 summing a wide range of latitude and longitude observations, reporting a global average  
122 value of  $10\pm 5$  ppbv, later updated to  $15\pm 5$ ppbv (Geminale et al. 2011). Geminale  
123 showed evidence of widespread temporal and spatial variability with indications of  
124 discrete localized sources (they found that methane is not uniformly distributed in the  
125 Martian atmosphere) and a summertime maximum of 45 ppbv in the north polar región.  
126 If true, these observations suggest that the variation of methane abundance is a feature  
127 of Mars from 2004 to 2008, although there is a high controversial about these detections  
128 due to instrument noise. The MeX measurements are obviously at the limits of the  
129 resolution and sensitivity of the PFS instrument, limited by the extremely poor spectral  
130 resolution that is  $\sim 200$  times the Mars methane linewidths (Webster et al. 2010; Zahnle  
131 et al. 2010). The data do not suffer from telluric contamination, but the spectral  
132 resolution is too coarse and the signals too weak for methane to be identified directly  
133 (Zahnle et al. 2010). Geminale estimates that a methane emission of 126 tons per year is  
134 required for the mentioned concentrations of  $\sim 10$  ppbv on Mars. This volume could rise  
135 up to 57,000 tons per year if the putative high methane of 45 ppbv observed from Earth  
136 are taken into account.

137 Mumma et al. (2009) (hereafter M09) applied infrared spectroscopic techniques  
138 using the powerful infrared high-resolution spectrometers NIRSPEC and CSHELL at  
139 high-altitude telescope observatories Keck-2 and NASA-IRTF respectively, to search  
140 for methane in the  $3.3 \mu\text{m}$  spectral region identifying multiple spectral lines having both  
141 spatial and temporal variability on the scale of several Mars years. The distinct spatial  
142 variability reported in M09 suggests regional source regions (Figure 1).

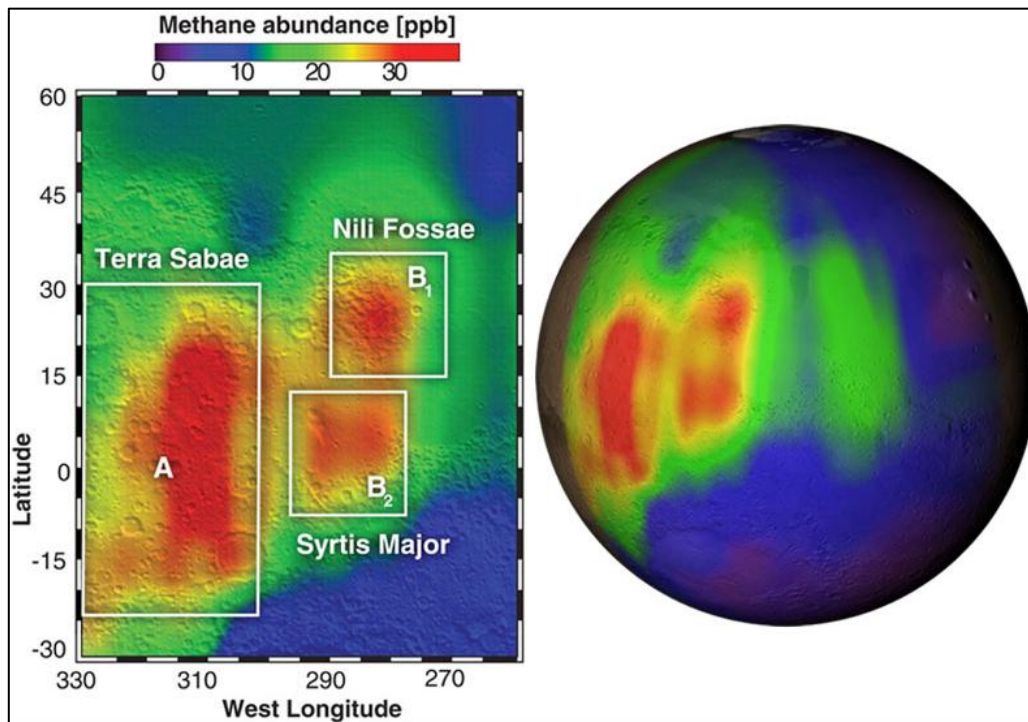


Figure 1. M09 observations of methane near the Syrtis Major volcanic district where methane appears notably localized (A, B<sub>1</sub>, and B<sub>2</sub>) in northern summer Ls 155°. Adapted from M09.

143  
144  
145

146 If true, methane is not just slowly leaking out everywhere, but there must be also  
147 large intermittent releases from specific areas.

148 Follow-up measurements (Villanueva et al. 2013) have failed to detect similar  
149 releases. The temporal variability could indicate seasonal variations in the source  
150 strength and, more surprisingly, extremely rapid destruction of methane through non-  
151 photochemical processes. There is no known mechanism for rapidly destroying methane  
152 chemically on Mars, although heterogeneous chemistry with surface peroxides and  
153 atmospheric aerosols, or destruction by peroxides generated intermittently through dust  
154 electrochemistry (Atreya et al. 2007) are possibilities. Such mechanisms would also  
155 likely disrupt the broader oxygen and hydrogen chemistry, and there is little evidence of  
156 such effects. Another analysis shows that methane in the wind can react with the  
157 eroded surface quartz grains (abraded silicates) which sequester methane by forming  
158 covalent Si-CH<sub>3</sub> bonds and thus an enrichment of the soil with reduced carbon, offering



159 a possible explanation for the fast disappearance of methane on Mars (Jensen et al.  
160 2014).

161 If the M09 values were accurate, the emission rate for the largest magnitude  
162 methane plume was estimated to be at least  $0.6 \text{ kg s}^{-1}$ , generating a mean mixing ratio of  
163 33 ppbv over the region of influence (approximately  $8,000,000 \text{ km}^2$ ) with a peak mixing  
164 ratio of 45 ppbv during north summer, and little methane outside this region. Were the  
165 contents of this plume to be spread uniformly over the globe, it would equate with a  
166 global average mixing ratio of 2 ppbv. Combined with other seasonally contiguous  
167 plumes that were also measured, the total global average methane abundance was  
168 estimated to be 6 ppbv. However, observations of the following Martian year found a  
169 mean mixing ratio of only 3 ppbv; thus M09 concluded that the chemical lifetime of  
170 atmospheric methane on Mars had to be less than 4 Mars years, and possibly as short as  
171 200 sols (far shorter than the photochemical lifetime of 350 years previously assumed).  
172 The conclusion that was drawn, then, was that methane is being removed from the  
173 atmosphere through means substantially more efficient than photochemical processes  
174 alone. M09 provided some limited analysis of plume evolution over time based upon  
175 the assumption of a diffusion-only atmosphere.

176 Zahnle et al. 2010 makes a strong case that the M09 detection was not martian  
177 methane at all, but the retrieval of a doppler shifted telluric line. The strongest reported  
178 signals using Earth based observations (Krasnopolsky et al. 2004 and M09) are from  
179 methane lines where the potential for confusion with other telluric or martian spectral  
180 features is significant, while observations at more favorable wavelengths indicate no  
181 methane above a 3 ppbv noise floor (Zahnle et al. 2010).

182 Fonti and Marzo 2010, using the thermal emission spectrometer (TES) on-board  
183 Mars Global Surveyor (MGS), showed evidence of widespread temporal variability  
184 with a global average value of 3 to 42 ppbv between 1999 and 2004 and with strong  
185 spatial variability in the methane signal intermittently present over locations where  
186 favorable geological conditions such as residual geothermal activity (Tharsis and  
187 Elysium) and strong hydration (Arabia Terrae) might be expected. There is considerable  
188 controversy about these detections, because TES lacks spectral line resolving power and  
189 requires to co-add nearly 3,000,000 of crude spectra to produce a very weak signal.  
190 Also, the identification of methane signal is controversial due to the presence of nearby  
191 H<sub>2</sub>O and CO<sub>2</sub> lines. The identification of methane depends on spatial and seasonal  
192 correlations with results from Geminale et al. (2008) and M09 (Z).

193 Other favorable locations for high methane levels are: Valles Marineris (42° to 7°N)  
194 with an upper limit of 10 ppbv and 3 ppbv outside that region (Krasnopolsky 2012), and  
195 with a value of 20±10 ppbv over Elysium region (Encrenaz 2008).

196 In an effort to minimize the previous problems reported (telluric contamination with  
197 other martian spectral features, instrument noise and very low spectral resolution data),  
198 observations were performed with the Echelon-Cross-Echelle Spectrograph (EXES)  
199 onboard the Stratospheric Observatory for Infrared Astronomy (SOFIA). The high  
200 altitude in the Earth atmosphere of SOFIA (~12-14 km) significantly reduces the effects  
201 of the terrestrial atmosphere allowing the use methane lines in the 7.5 μm band. These  
202 measurements suggest an upper limit on the methane volume mixing ratio range from 1  
203 to 9 ppbv (Aoki et al. 2017, 2018). The measurements were performed at northern  
204 summer (Ls 123°) of Mars year 33.

205 Based on current understanding, the total photochemical loss rate of methane in the  
206 martian atmosphere is  $2.2 \times 10^5 \text{ cm}^{-2} \text{ s}^{-1}$ , and its lifetime is 340 years (Krasnopolsky et al.  
207 2004). Since the vertical and horizontal mixing time is much shorter than the  
208 photochemical lifetime, methane should be uniformly mixed and distributed throughout  
209 the atmosphere. However, the different methane observations (Table 1) indicate a  
210 temporal and spatial variability of methane that is inconsistent with a well mixed  
211 atmosphere or inconsistent with a long photochemical lifetime (Lefevre and Forget  
212 2009). Further, with a long photochemical lifetime, even episodic emissions like those  
213 identified in Table 1 would result in a large global methane abundance.

214 Another possibility is that martian photochemical models could be wrong (Cesar  
215 Menor-Salván, personal communication), because the rapid destruction of methane is  
216 very difficult to reconcile with the known distribution of other gases in the Mars  
217 atmosphere. Methane oxidation would deplete the oxygen in Mars atmosphere in less  
218 than 10,000 years unless balanced by an equally large unknown source of oxidizing  
219 power. Perchlorates on the surface and on atmospheric dust, or the production of  $\text{H}_2\text{O}_2$   
220 through electrochemical processes in dust devils and dust storms might be able to  
221 provide oxidation source (Atreya et al. 2007). Photochemical removal of methane also  
222 disrupts the hydrogen chemistry and those effects would presumably be seen in other,  
223 more obvious places on Mars (e.g., water, OH,  $\text{O}_2$ ,  $\text{O}_3$ , and CO/ $\text{CO}_2$  abundance). The  
224 effects on other species has not been observed, although there are unexplained  
225 variations in  $\text{O}_2$  (McConnochie) that might provide some clues. Some colleagues  
226 (Moore 2017) proposed that the small seasonal variations of methane background  
227 values could be traced to seasonal variations in UV, but UV insolation does not change  
228 that much over the seasons at the equatorial location of Gale crater, and it cannot

229 explain the decrease from the peak values back to the background level.  
230 Photochemical activity might be expected to rise and fall slightly with the seasons, but  
231 the slight variations are insufficient to produce the necessary and sudden destruction  
232 mechanisms.

233 To the extent that SAM and perhaps other MSL instrumentation can measure trace  
234 gases, particularly those species whose presence are less controversial than methane, the  
235 seasonal and diurnal variability and abundance could provide further clues about the  
236 mixing time scale of the crater. Oxygen species (O, O<sub>2</sub> and/or O<sub>3</sub>) are potential  
237 candidates for investigation, as is CO. Whether other trace gases (for example radon,  
238 which has a uniquely subsurface source) exhibit peculiar behaviors has yet to be  
239 determined, but it is an interesting topic to consider for the future.

## 240 **1.2 SAM methane detections at Gale crater**

241 In situ measurements provide ground truth using direct and, in principle, more  
242 reliable methods than those from Earth or Mars orbit. The Tunable Laser Spectrometer  
243 (TLS) of the Sample Analysis at Mars (SAM) instrument suite aboard the MSL  
244 Curiosity rover at Gale crater (Mars) was specifically designed to obtain precise  
245 abundance measurements, including the potential measurement of different  
246 isotopologues of methane, using laser absorption spectroscopy (Table 1).

247 SAM determines methane abundances by taking the difference between  
248 measurements from a cell with an atmospheric sample and an empty cell. Using this  
249 difference technique minimizes the effect of potential contamination between  
250 measurements, and atmospheric methane would be detected as the difference between  
251 the signals (Webster et al. 2015).

252 During the long pre-launch activities in Florida, the evacuated foreoptics chamber  
253 leaked up to a significant pressure (~76 mbar) by the time MSL Curiosity rover arrived  
254 at Mars. This pressure included terrestrial “Florida air” from the launch site that  
255 contained significant terrestrial methane gas (~10 ppmv) (Webster et al. 2015 SM). This  
256 concentration is ~1,000 times the ppbv values that SAM has since measured in the  
257 martian atmosphere. Zahnle (2015) expressed the possibility that the Curiosity rover  
258 itself has known or hidden sources of methane that might contaminate the TLS-SAM  
259 foreoptics chamber to produce methane around the rover. In order to rule out this, the  
260 SAM team measured the foreoptics pressure every time the instrument was running, and  
261 apart from two deliberate attempts to reduce that pressure (pump out the chamber),  
262 there is no evidence of a broken seal or leakage of gas out of the foreoptics chamber  
263 over the 5 years of measurements. Second, with the previously mentioned “difference  
264 method”, the “empty cell” spectra/measurements provide a direct measurement of the  
265 foreoptics methane amount, which has varied somewhat during pumping attempts, but  
266 remains around ~1015 molecules of methane in the foreoptics chamber.

267 Two different atmospheric sampling methods are used by SAM. The first is a  
268 “direct ingest” method in which gas is ingested into the instrument through an inlet port  
269 located on the side of the Curiosity rover, taking ~10 minutes to fill to ~7 mbar and  
270 producing uncertainties of ~2 ppbv for each measurement. The second is an  
271 “enrichment” method, that ingests atmospheric gas through a second inlet port, which is  
272 passed over a CO<sub>2</sub> scrubber to more slowly fill the instrument (~2 hours) to ~7 mbar  
273 (Webster et al. 2015). This method efficiently removes the incoming CO<sub>2</sub> and  
274 effectively enriches the methane abundance by a factor of ~25, allowing more precise  
275 measurements of low background levels. In both cases, the time of initiation of

276 measurements is constrained by competing rover activities and power availability.  
277 Most of the SAM-TLS measurements were acquired during nighttime (except on sols  
278 305 and 525) due to thermal requirements of the SAM sample handling system. Also,  
279 long periods of time can pass between measurements.

280 The record of SAM methane measurements is shown in Figure 2. The first four  
281 measurements (Sols 79, 81, 106 and 293 after MSL Curiosity rover landing) indicated a  
282 value of <1.5 ppbv using the direct ingestion method (see Table 2). Measurements  
283 taken shortly thereafter were consistent with this initial measurement (Webster et al.  
284 2015). Another measurement taken almost 200 sols later was also at the 1 ppbv level.  
285 There is no way to know if methane concentrations remained consistently at this level  
286 during this period, despite the green bar in the Figure 2 that incorrectly suggests such  
287 knowledge.

288 A spike in methane abundance was first noted at sol 467 (Ls 55°). It is commonly  
289 assumed that methane abundance remained continuously elevated between sol 467 and  
290 526 (~Ls 55-82°), with a mean value of  $7.2 \pm 2.1$  ppbv (95% CI) (Webster et al. 2015),  
291 but there are no data to support this assumption. The infrequency of methane  
292 measurements introduces great uncertainty about variations between spikes, because it  
293 is not known precisely when the spikes began, how long they lasted, or how long it took  
294 for the values to return to background values. It could be possible that the methane  
295 values come back to background values in hours or sols after the peak, and the detected  
296 spikes were serendipitous.

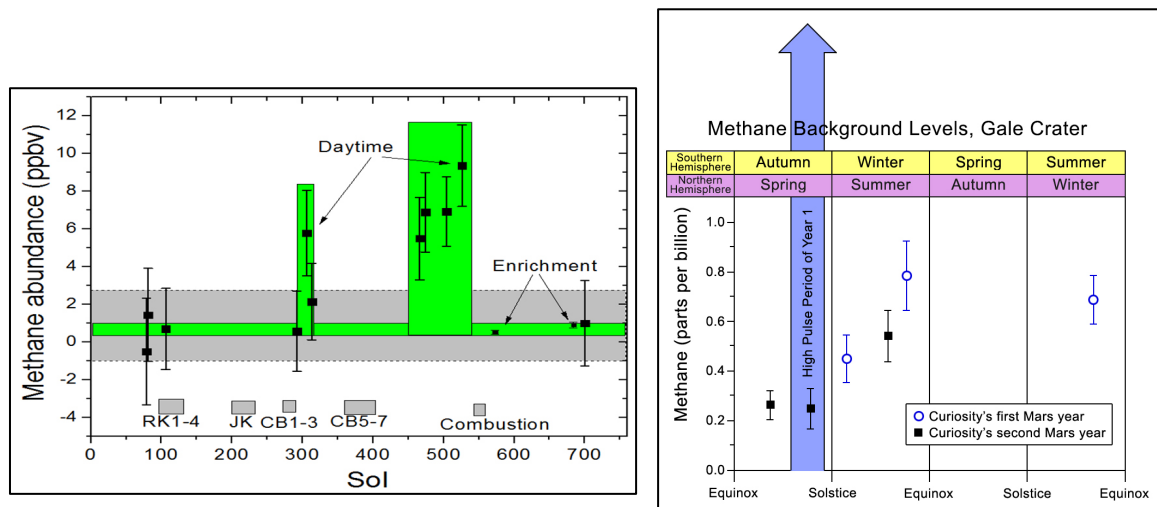


Figure 2. Two years of subsequent measurements taken during the rover's journey of 9 km over highly varied terrain. SAM methane measurements fall into two basic categories: larger spikes of up to ~7 ppbv (left) and low level background abundance of ~0.3-0.7 ppbv (right). The background measurements may indicate a seasonal cycle. The time between measurements is insufficient to determine how frequently spikes in abundance occur, how fast they decay, or how common the spikes may be. The green shading incorrectly suggests knowledge of methane concentrations at times when no measurements were taken. [Mars Exploration Program NASA website December 16, 2014 (left image) and May 11, 2016 (right image)].

297

298

299

300 measurement was taken at sol 573 using the enrichment method. Subsequent  
 301 measurements at sol 684 (both direct ingest and enrichment method) were also at the  
 302 background level.

303 Neglecting the spikes of concentration, there appears to be a seasonal cycle in  
 304 the background methane concentrations at Gale crater (Figure 2), with a mean value of  
 305 ~0.4 ppbv (compared with 1.8 ppmv on Earth, the background methane content at Gale  
 306 crater is 4,500 thousand times less), ranging from a minimum about 0.3 ppbv near the  
 307 northern summer solstice to a peak about 0.7 ppbv sometime between the northern  
 308 autumn equinox and the winter solstice (Webster et al 2017).

309

310

311

312  
313

**Table 2. MSL Curiosity rover TLS-SAM methane measurements at Gale crater over a ~20-month period (from Oct. 26th 2012 to July 9th 2014). Adapted from Webster et al. 2015.**

Run Description	Sol	Ls deg	Mean CH <sub>4</sub> value ± SEM (ppbv)
DIM1	79.96	195.60	-0.51±2.83
DIM2	81.89	196.77	1.43±2.47
DIM3	106.14	211.74	0.68±2.15
DIM4	293.16	329.16	0.56±2.13
DIM5	305.58	336.12	5.78±2.27
DIM6	314.14	340.83	2.13±2.02
DIM7	467.14	55.59	5.48±2.19
DIM8	475.14	59.20	6.88±2.11
DIM9	505.12	72.66	6.91±1.84
DIM10	525.56	81.84	9.34±2.16
EM1	573.08	103.48	0.47±0.11
EM2	684.06	158.61	0.90±0.16
DIM11	684.27	158.73	0.99±2.08

315

316

317

318

319

320

321

Is important to note that all the martian methane detections reported since 2009 (Krasnopolsky 2011; Krasnopolsky 2012; Villanueva et al. 2013; Webster et al. 2013; Webster et al. 2015 and Aoiki et al. 2018) are <9 ppbv or below detection thresholds altogether. Also, many of the earth-based and orbital detections are an order of magnitude greater than the SAM background, which is odd considering the sporadic nature of the remote measurements.

322

### **1.3 Previous modeling works of methane transport**

323

324

325

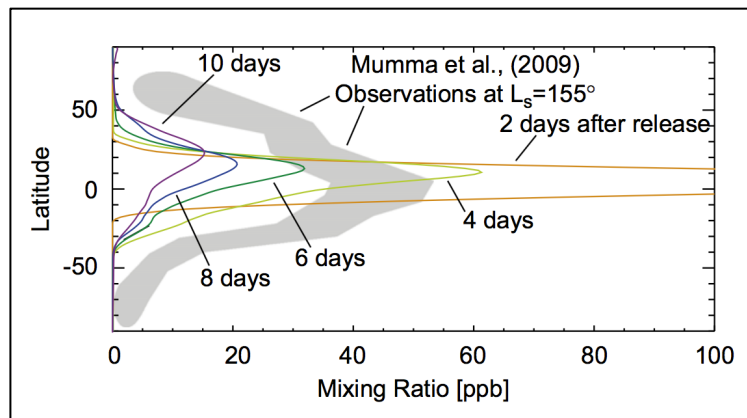
326

327

328

Previous works modeling martian methane plumes have been undertaken using GCMs: Mishna et al. 2011, Holmes et al. 2015 and Viscardy et al. 2016. Mishna et al. 2011 concluded that a best match to observations would be found if a nearly instantaneous (rather than gradual), spatially large release occurred just before the time of observation (before it could be substantially diluted) no more than 1–2 sol earlier (Figure 3). This result is consistent with relatively fast atmospheric mixing.





329  
 330 **Figure 3. Latitudinal distribution of plume mixing ratio as a function of time for central longitude of**  
 331 **315°W, and 16°x10° (lon, lat) smoothing. Each curve (progressing from right to left) shows the**  
 332 **variation in 2 sol increments, from 2 sols after a ‘pulse’ release (rightmost) to 10 sols after (leftmost).**  
 333 **The shaded region encloses the M09 methane observations. Adapted from Mischna et al. 2011.**

334         The results of Holmes et al. 2015 show that the spatial and temporal variability  
 335 of methane on Mars implied by observations might be explained by advection from  
 336 localized time-dependent sources alongside a currently unknown methane sink. The best  
 337 agreement between the existing observations is found in their simulations using a steady  
 338 state release from a small source over Nili Fossae. Holmes et al. 2015 suggest that the  
 339 lower levels of SAM measurements when compared to previous results (M09 and Fonti  
 340 and Marzo 2010) can be explained by a relative lack of, or indeed complete absence of,  
 341 methane source emission in the intervening period. Again, this requires a hitherto  
 342 unknown large methane sink.

343         Previous GCM simulations have focused on the horizontal evolution of the  
 344 methane, but Viscardy et al. 2016 explored the three-dimensional dispersion of methane  
 345 throughout the atmosphere after a surface release. Their simulations show that surface  
 346 emissions of methane results in a non-uniform vertical distribution, including the  
 347 formation of elevated layers, shortly after the release. As expected, the destination of  
 348 the released methane is determined by the global circulation pattern at the time of the  
 349 release, and the methane can be transported to locations over the planet that are far

350 away from the emission place. It typically takes several weeks for the methane to  
351 become uniformly mixed, implying that the detection of vertical layers of methane can  
352 be a clue of recent surface emission. Their finding shows abundances of methane higher  
353 up in the atmosphere can be much larger than those measured at the surface where the  
354 rover Curiosity is located.

355         As shown by Pla-Garcia et al. 2016 and Rafkin et al. 2016 (hereafter PGR16)  
356 the circulation in and around the ~150 km diameter Gale crater is very complex, with  
357 strong seasonal and diurnal variations. The expectation is that the distribution of  
358 methane in and around the crater will be strongly influenced by the complex  
359 circulations. In order to represent the large scale release and dispersion of methane, the  
360 use of a GCM, as done in the previous works (Mischna et al. 2011, Holmes et al. 2015  
361 and Vicardy et al. 2016) is appropriate, but a GCM cannot capture the transport in and  
362 around Gale crater. The mesoscale circulations driven by the complex topography at the  
363 scale of the crater can only be simulated by a model with significantly greater spatial  
364 and temporal resolution. The work herein extends PGR16 to investigate the transport  
365 and dispersion of methane by resolved crater circulations.

366         It is difficult to explain the SAM and previous measurements at the global scale  
367 using global scale models. An individual peak methane detection could be consistent  
368 with a regional release and large scale transport, but continuously elevated peaks are  
369 not. For methane to remain elevated for many sols, a release would have to be nearly  
370 continuous in order to counteract transport. Such a continuous release would then result  
371 in globally large methane values after the relatively short mixing timescales.

372         The behavior of highly localized releases (on the scale of Gale crater or smaller)  
373 or the transport of a larger release by the complex circulations in Gale Crater, has yet to

374 be fully explored. For example, PGR16 hypothesized that gases released in the crater  
375 could become trapped in the lowest portion of the crater basin due to the very cold and  
376 dense air mass that would be resistant to mixing with air above. Cold air trapping is a  
377 common phenomena on Earth and often results in the build up of pollution in enclosed  
378 basins (e.g., Malek et al. 2006, Whiteman et al 2001, Steyn et al 2013).

## 379 **2 Mars methane modeling experiments**

### 380 **2.1 Mars Regional Atmospheric Modeling System (MRAMS)**

381 The Mars Regional Atmospheric Modeling System (MRAMS) is used in this study to  
382 investigate the transport and dispersion of trace gases in and around Gale crater.  
383 MRAMS is a versatile numerical mesoscale model that simulates the circulations of the  
384 Martian atmosphere at regional and local scales (Rafkin et al. 2001, 2002, 2006, 2009;  
385 PGR16). MRAMS is derived from the Regional Atmospheric Modeling System  
386 (RAMS) which is a widely used nonhydrostatic Earth mesoscale and cloud-scale model  
387 (Pielke et al., 1992) designed to simulate synoptic-scale, mesoscale, and microscale  
388 atmospheric flows over complex terrain. MRAMS is explicitly designed to simulate  
389 Mars atmospheric circulations at the mesoscale and smaller scales with realistic, high-  
390 resolution surface properties.

391 To simulate the Gale crater meteorological environment, MRAMS is configured  
392 with five grids centered over the MSL Curiosity rover site (Figure 2; PGR16). The  
393 grids are configured, as much as practicable, to cover topographic regions that might  
394 influence the solution on a particular grid. The outermost grid (the mother domain),  
395 extends well into the northern hemisphere, covering the north polar cap and the  
396 hemispheric topographic dichotomy. This configuration can capture the strong

397 topographic flows that sometimes occur near the hemispheric dichotomy, and it can  
398 capture the seasonal mean meridional flows (i.e., the Hadley Cell) that are nearly global  
399 in extent and that should have a great impact into the methane mixing. Grids are also  
400 specified so as to minimize, as much as possible, the crossing of large topographic  
401 features at the boundaries, which can create spurious noise. The horizontal grid spacing  
402 at the center of the five grids are 240, 80, 26.7, 8.9 and 2.96 km respectively (Figure 2;  
403 PGR16), with the innermost grid centered at the location where SAM detected the  
404 methane spikes.

405 All the grids have the same vertical grid configuration with the vertical winds  
406 staggered between thermodynamic levels. The lowest thermodynamic level (where  
407 temperature and pressure are prognosed) is ~14.5 m above the ground. Ideally, the first  
408 vertical level would be located at the height of the TLS-SAM sensor (~1 m), but this is  
409 not computationally practical; the integration time step for nonhydrostatic models is  
410 closely coupled to the thickness of that layer. Using a lowest model thickness of one to  
411 two meters would have required a mother domain time step of fractions of a second  
412 compared to a value closer to 10 s. Thus, the model would have run approximately two  
413 orders of magnitude slower. This vertical spacing is gradually stretched with height  
414 until reaching a maximum spacing of 2,500 m, and the levels gradually transition from  
415 terrain-following near the surface to horizontal at the top of the model. The spacing  
416 does not exceed 100 m in the lowest 1 km, and does not exceed 400 m in the lowest 4  
417 km. The model top is 51 km with 50 vertical grid points.

418 Output from the NASA Ames General Circulation Model (Kahre et al. 2006) is  
419 used to initialize the atmospheric state in MRAMS. Time-dependent boundary  
420 conditions are also supplied from the NASA model output at intervals of 1/16th of a sol.

421 This frequency is sufficient to capture the thermal tide signal, but some amount of  
422 aliasing is possible. Dust is prescribed based on zonally-averaged TES retrievals (in  
423 non-global dust storm years) and follows a Conrath-v profile in altitude (Conrath,  
424 1975). The Conrath-v parameter that describes the depth of the dust varies with season  
425 and latitude as prescribed in the baseline version of the Ames GCM. The deepest  
426 atmospheric dust column is found near the subsolar latitude. CO<sub>2</sub> ice is placed on the  
427 surface based on the location predicted by the GCM at the MRAMS initial time. The  
428 ice is static in time during the MRAMS integration; the active CO<sub>2</sub> cycle is disabled,  
429 which is a valid assumption for the short periods of simulation time ( $\leq 12$  sols) under  
430 consideration with the model. MRAMS surface properties are obtained from TES  
431 thermal inertia (nighttime) and albedo data sets binned at 1/8th of a degree, and from  
432 MOLA topography binned at 1/128th of a degree (Table 1). The model computes  
433 topographic shadowing and slope radiation effects based on the MOLA data.

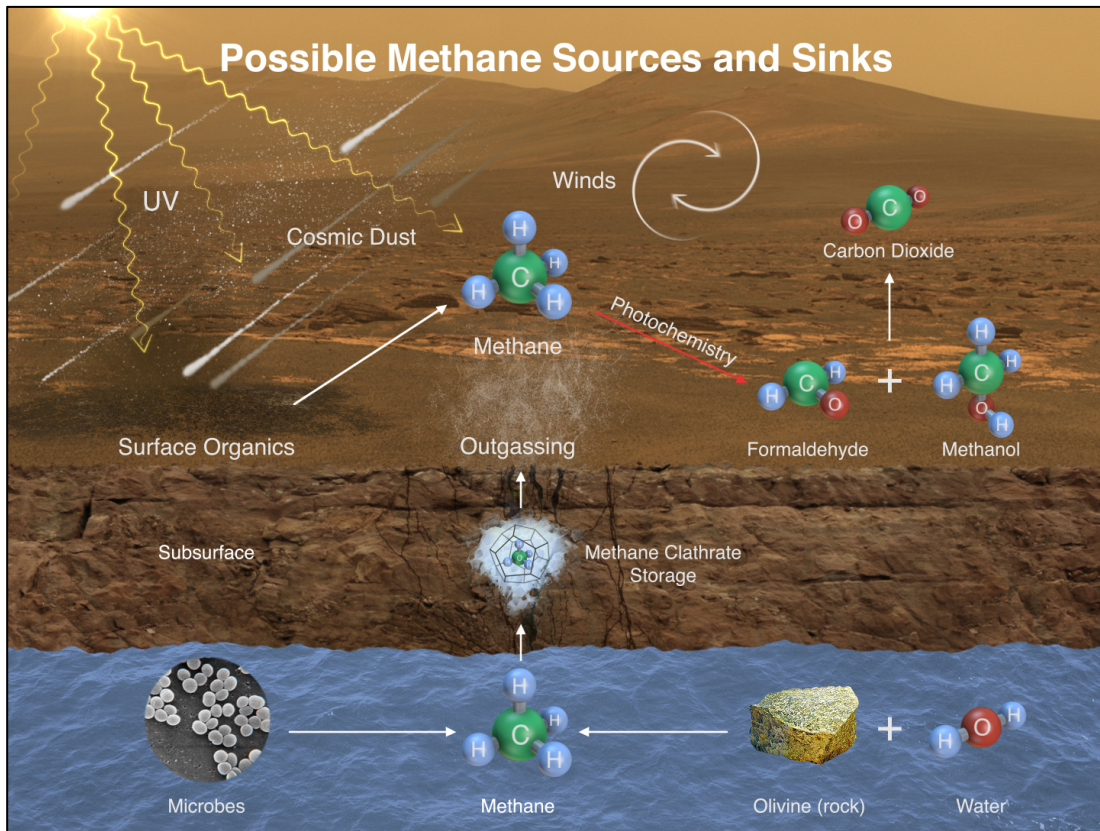
434         The model was run for twelve sols. Although the circulation patterns are highly  
435 repeatable from sol to sol beginning within a few hours of initialization, the first sol  
436 may be regarded as “spin-up”. All simulations were started at or slightly before local  
437 sunrise. In order to characterize seasonal mixing changes throughout the Martian year,  
438 simulations were conducted at Ls 270° (the wholesale inundation of the crater period),  
439 Ls 90° (as a representative of the rest of the year) and Ls 155° (the season of the 2003  
440 Earth-based detections M09). Using the above model configurations, PGR16  
441 demonstrate that the model was able to reproduce the meteorological observations  
442 obtained by the MSL Curiosity rover REMS instrument (Gomez-Elvira et al. 2012) in  
443 Gale crater.

444 MRAMS has the capability to simulate the transport of inert gases as tracers,  
445 and this capability is used to represent the transport of mixing of methane. An  
446 atmospheric tracer may be considered as an inert gas released into the model  
447 atmosphere and which is transported by advection and dispersion (subgrid turbulent  
448 mixing). Since the photochemical lifetime of methane is thought to be very long  
449 compared to the 10 sols duration of the simulation, no sinks are imposed on the tracers  
450 that represent methane (Lefevre and Forget 2009). Tracers in the MRAMS model can  
451 be placed anywhere, and may be released instantaneously or at a user-specified, time-  
452 dependent rate. Tracers are not radiatively active and do not contribute to the tendency  
453 of any model prognostic variables. Tracers released from the same location but with  
454 different emission fluxes will evolve identically with abundances in proportion to their  
455 source fluxes. In other words, the source flux may be scaled after numerical integration  
456 in order to get a proportional answer (e.g. multiplying the flux in MRAMS by 200  
457 produces a 200 times higher tracer mixing ratio value but with an otherwise identical  
458 spatial pattern).

## 459 **2.2 Martian clathrates subsurface model**

460 The detection of methane variability necessitates a methane source (Figure 4). These  
461 sources could include non-biological processes like as serpentinization of olivine (Oze  
462 and Sharma 2005; Atreya et al. 2007), geothermal production (Etiope et al. 2011),  
463 erosion of basalt with methane inclusions (McMahon et al. 2013), release from regolith-  
464 absorbed gas (Meslin et al. 2011; Gough et al. 2010), exogenous sources to include  
465 infall of interplanetary dust particles (IDP) and cometary impact material (Schuerger et  
466 al. 2012), biological sources like subsurface methanogen microorganisms  
467 (Krasnopolsky et al. 2004) or release of methane from organic decay in solution

468 (Keppler et al. 2012; Schuerger et al. 2012; Poch et al. 2014). The evidence for each of  
469 these sources is generally weak or speculative.



470

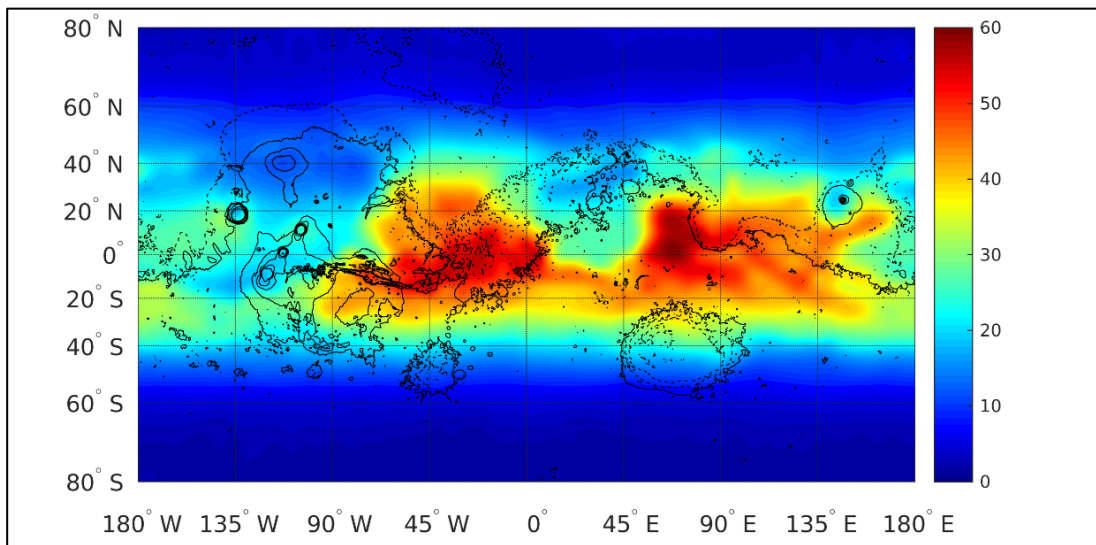
471 **Figure 4. Possible methane sources and sinks on Mars. Image credit: NASA/JPL-CALTECH**

472 The Mars methane gas produced by these sources could be trapped in subsurface  
473 clathrates. Clathrate hydrates are crystalline compounds comprised of cages formed by  
474 hydrogen-bonded water molecules inside of which guest gas molecules are trapped. An  
475 increase in temperature or a decrease in pressure can lead to the dissociation of  
476 clathrates, which results in the release of the trapped gas. Under colder conditions of an  
477 earlier climate period (e.g., resulting from obliquity cycles), a cryosphere could trap  
478 methane as clathrates in stable form at depth. Under current climate conditions those  
479 same clathrates could become unstable and result in a sporadic release. Previous studies  
480 (Chastain et al. 2007) indicate that the present-day conditions in the martian subsurface  
481 are favorable for the presence of clathrates.

482           Since methane fluxes need to be imposed in the MRAMS simulations, it is  
483 beneficial to utilize an emission rate that is representative of at least one plausible  
484 martian source mechanism. Methane clathrates are selected for this purpose. The  
485 assumption of a clathrate source for the MRAMS simulations is purely a convenience  
486 since reasonable estimates for a surface methane flux can be obtained. Recalling that the  
487 MRAMS tracer abundance scales linearly with the flux, the solution for any desired flux  
488 magnitude can be obtained from the MRAMS results, regardless of the actual flux  
489 mechanism.

490           Our colleagues Özgür Karatekin and Elodie Gloesener produced maps of  
491 methane-rich clathrate stability zones (Figure 5) obtained by coupling the stability  
492 conditions of methane clathrate with a subsurface model (Karatekin et al. 2016;  
493 Karatekin et al. 2017; Gloesener et al. 2017, hereafter KG17). Ancient clathrates may  
494 exist at depth where the geothermal gradient causes them to decompose over time  
495 (Stevens et al., 2015). The regolith properties directly control the subsurface thermal  
496 conditions and therefore the depth of clathrate stability: the lower the thermal inertia in  
497 the surface, the less stable the clathrates will be (the thermal wave penetrates more  
498 deeply). This map, based on the mean annual temperature and TES-derived thermal  
499 inertia among other variables, does not reveal local scale variations, so if Gale crater  
500 was formed after the emplacement of the clathrates, it is possible that there could be  
501 methane locally closer to the surface than would be inferred from this map.

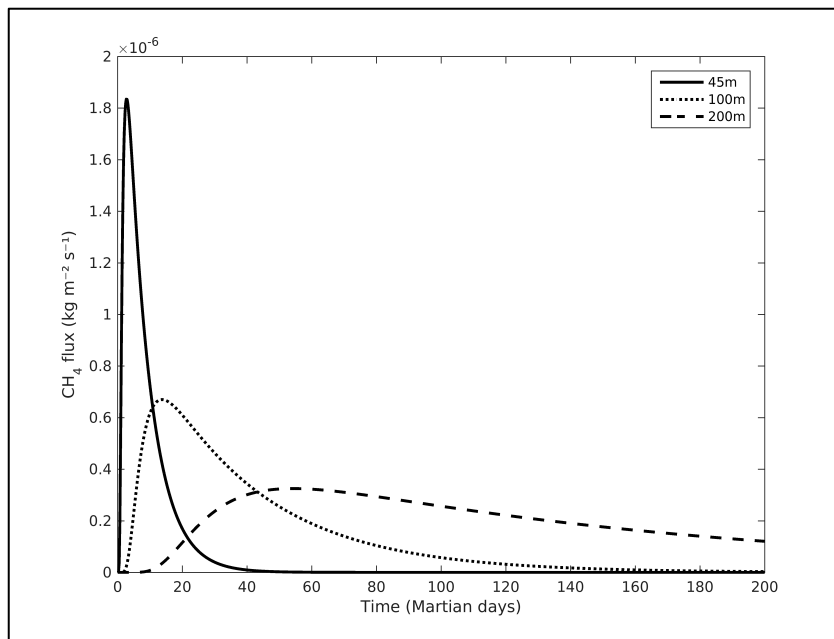




502 **Figure 5. Depth (m) of the beginning of hydrate stability zone in present-day martian subsurface for**  
 503 **clathrates formed from a gas phase with 90% fraction of methane. Adapted from Gloesener et al. 2017**  
 504 **and Karatekin et al. 2017**  
 505

506 Methane clathrates can be stable very near the surface at high latitudes, and can  
 507 be as close as 20 m to the surface in the tropics under today's climate. In the cases  
 508 where a surface flux of methane is specified in the MRAMS simulations, the flux is  
 509 assumed to come from subsurface methane clathrate emplaced in earlier geological  
 510 times and which has been destabilized due to changes in the regolith energy balance.  
 511 KG17 calculated the surface methane flux by modeling methane gas transport through  
 512 the regolith to the surface via molecular and Knudsen diffusion. Gas adsorption  
 513 processes are ignored in these calculations of the methane flux used in the MRAMS  
 514 experiments. Including adsorption reduces the methane flux by roughly  $\sim 30$  times,  
 515 although it increase the emission time in the same amount amplifying seasonal  
 516 variations of background methane through Arrhenius dependency. The dissociation of 1  
 517  $\text{m}^3$  of clathrates formed from a gas phase containing 90% of methane at a depth of 45 m  
 518 in Gale crater (assuming a mean thermal inertia of  $\sim 365$  for the first meters and  
 519 increasing with depth), produces  $\sim 2 \times 10^{-6} \text{ kg m}^{-2} \text{ s}^{-1}$  methane flux at Ls 285° (Figure 6)  
 520 during the first sols. It is important to note that, although the methane flux should be

521 higher during warmer seasons due to the dependence in temperature of the diffusion  
522 coefficient (and the kinetic constant if you take into account adsorption), the same value  
523 is used for all the seasons modeled in MRAMS (Ls 90°, Ls 155° and Ls 270°), so  
524 methane flux in our simulations is overestimated for Ls 90° and Ls 155°. New  
525 experiments are being performed with updated methane flux values.



526

527 **Figure 6. Methane flux for clathrates formed from a gas phase with 90% of methane derived from**  
528 **Gloesener et al. 2017 subsurface diffusive model that includes molecular and Knudsen diffusion.**

### 529 **2.3 MRAMS methane experiment scenarios**

530 Different MRAMS tracer scenarios were constructed with simulations at different  
531 seasons (Ls 90°, 155° and 270°) as shown in table 3.

532 The punctual methane release scenarios are designed to quantify the rate of  
533 mixing within the crater and between the crater and air outside the crater.

534 The steady state methane release scenarios explore the transport of methane  
535 under specific flux scenarios and, location and areal extent of the emission. The  
536 selection of these seasons is based on our previous work (PGR16). Ls 270° is  
537 anomalous in that it is a very windy season with large amplitude breaking mountain

538 waves, and rapid mixing with air external to the crater was inferred. The regional  
 539 northwest winds from northern lowlands scour the very bottom of the crater floor.  
 540 Crater circulation is pushed and extended dramatically to the south. This is not just air  
 541 flowing through topographic passes like Peace Valles, rather it is a wholesale  
 542 inundation of the crater from the air to the northwest. Based in our previous PGR16  
 543 work, Ls 270° is presumed the fastest exchange period between air inside and outside  
 544 crater during Mars year and during the other seasons the mixing were presumed slower.  
 545 In the rest of the year other than Ls 270°, mixing between the crater air mass and the  
 546 external crater air was interpreted to be more subdued. Ls 90° was selected for our  
 547 methane mixing experiments because it is representative of most rest of the year.  
 548 Simulations at Ls 155° were also conducted, because it is the season of the M09 2003  
 549 Earth-based detections.

<b>CH<sub>4</sub> release</b>	<b>Punctual emission</b>	<b>Steady state emission</b>
<b>Inside</b> crater small size area emission (~149 km <sup>2</sup> ) close to MSL location	<b>Ls90 &amp; Ls270</b>	<b>Ls90 &amp; Ls270</b>
<b>NW Outside</b> crater medium size area emission (~6,400 km <sup>2</sup> )	<b>Ls90 &amp; Ls270</b>	<b>Ls90 &amp; Ls270</b>
<b>NE&amp;SW&amp;SE Outside</b> crater medium size area emission (~6,400 km <sup>2</sup> )	X	
<b>M09</b> large size area (~8,000,000 km <sup>2</sup> )	X	<b>Ls90, Ls155 &amp; Ls270</b>
<b>M09</b> large size area (~2,000,000 km <sup>2</sup> )	X	<b>Ls270</b>

550

551 **Table 3. MRAMS methane punctual and steady state release scenarios for inside and outside Gale**  
 552 **crater release locations at Ls 90° , Ls 155° and Ls 270° .**

553 **2.3.1 Punctual methane release scenarios**

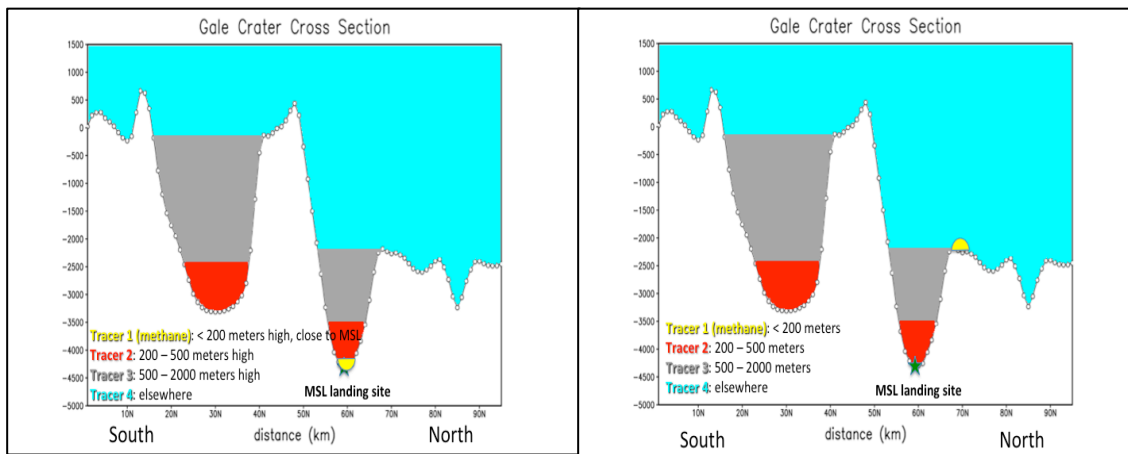
554 The goal of punctual in time methane release experiments is to study how the different  
 555 air masses containing each of the tracers mix with one another. The amount of mixing  
 556 can be diagnosed by looking at the fraction of each tracer compared to all the tracers.

557 Fraction of a tracer X is  $\frac{\text{tracer } X}{\sum \text{all tracers}}$ . For example, at the start, 100% of the tracers in the  
558 bottom (<200 m high) of the crater are tracer #1 mimicking methane, because there has  
559 yet to be any mixing. If at some later time it is found that 50% of the tracers in the  
560 bottom of the crater are tracer #1, then half of that original air mass has been mixed  
561 away. By looking at the fraction of other tracers, the amount of mixing with each of the  
562 different air masses can be determined.

563 In these experiments, four tracers were strategically placed into the model after  
564 spin-up (1 sol) to diagnose the mixing of air inside and outside the crater both for Ls 90°  
565 and Ls 270° seasons. There were no additional sources (no flux) or sinks of tracers  
566 (photochemical lifetime destruction is orders of magnitude higher than our twelve sols  
567 simulation). Tracer #1 represents a hypothetical methane-enriched air mass near the  
568 surface (<200 m high). The other three tracers are placed in different layers above tracer  
569 #1 (Figure 7) in order to track those air masses. Tracer #2 is placed from 200 to 500 m  
570 above ground level (hereafter AGL) inside Gale crater, tracer #3 from 500 to 2,000 m  
571 AGL inside Gale crater, and tracer #4 elsewhere (outside and above Gale crater).

572 In the punctual methane release inside of Gale crater experiment (Figure 7, left  
573 side), tracer #1 have an area of ~149 km<sup>2</sup> and is located one grid point (less than 3 km)  
574 west from the MSL Curiosity rover in the north crater basin.

575 In the punctual methane release outside of Gale crater experiment (Figure 7,  
576 right side), tracer #1 have an area of ~6,400 km<sup>2</sup> and is located ~100 km northwest  
577 upstream of the landing site outside the crater.

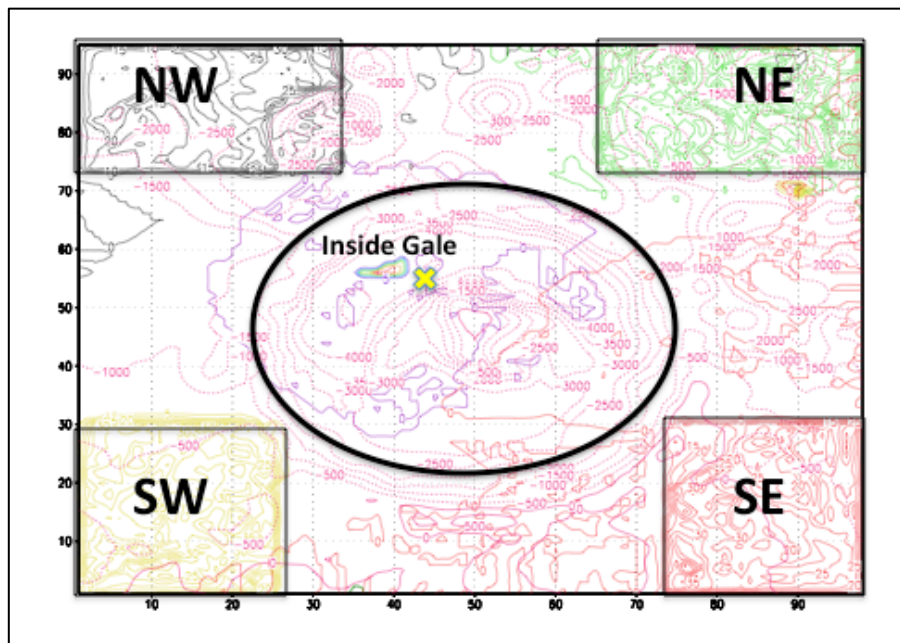


578

579 **Figure 7. Punctual methane release scenarios cross sections (Mt. Sharp in the middle, north basin in the right and south basin in the left in both boxes). Tracer #1 (yellow) is placed one grid point (less than 3 km) west from the MSL Curiosity rover location inside Gale crater (left box) and ~100 km northwest upstream of the MSL landing site (right box). In both cases, Tracer #1 is placed <200 m AGL, Tracer #2 (red) is placed from 200 to 500 meters high, Tracer #3 (grey) from 500 to 2,000 m AGL inside Gale crater, and tracer #4 (blue) elsewhere (outside and above Gale crater).**

### 585 2.3.2 Steady state methane release scenarios

586 In these scenarios, the methane release is steady state in time (continuous surface  
 587 emission) with a prescribed flux of  $\sim 2 \times 10^{-6} \text{ kg m}^{-2} \text{ s}^{-1}$  during a period of twelve sols.  
 588 Five independent methane steady state release sources, four of them located ~100 km  
 589 NW, NE, SW and SE upstream of the MSL Curiosity rover landing site outside the Gale  
 590 crater with an area of  $\sim 6,400 \text{ km}^2$  each and another one located inside of the crater ~1  
 591 grid point west from the rover with an area of  $\sim 149 \text{ km}^2$ , as shown in Figure 8. Since  
 592 the tracers do not interact with each other, multiple tracer configurations can be studied  
 593 simultaneously in a single simulation.



594

595 **Figure 8. Steady state methane release scenarios aerial view. Gale crater encircled. The yellow cross**  
 596 **represent the MSL Curiosity rover location. Four independent methane release sources were located**  
 597 **outside the crater ~100 km NW, NE, SW and SE upstream of the rover landing site with an area of**  
 598 **~6,400 km<sup>2</sup> each and another one was located inside of the crater ~1 grid point west from the rover**  
 599 **with an area of ~149 km<sup>2</sup>**

600 Two additional experiments were performed mimicking M09 release areas,  
 601 including the “full” M09 release area (~8,000,000 km<sup>2</sup>) source at Terra Sabae (A in  
 602 Figure 1), Nili Fossae (B<sub>1</sub> in Figure 1) and Syrtis Major (B<sub>2</sub> in Figure 1) and a “partial”  
 603 M09 release source only at Nili Fossae area (~2,000,000 km<sup>2</sup>).

### 604 **3 Results**

605 To gain a true appreciation for the complexity, beauty and evolution of methane  
 606 emissions at various locations, the reader should proceed no further without first  
 607 viewing the animations of the circulations provided in the supplementary material.

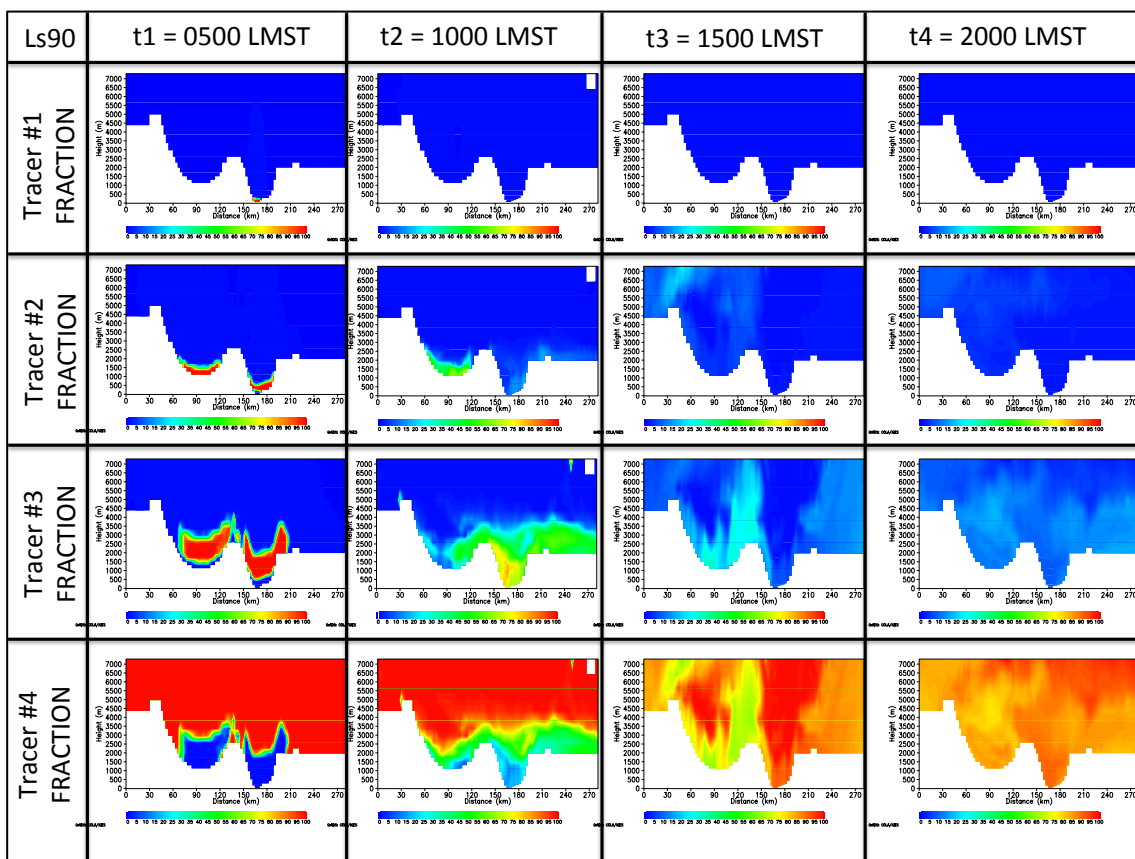
608 Again and as discussed in the MRAMS model description section, the lowest  
 609 thermodynamic level where methane could be sampled in our simulations is ~14.5 m  
 610 above the ground due to computational restrictions, so higher methane values at SAM  
 611 high (~1 m) compared to the methane values sampled with MRAMS are expected.

612 It is important to note that the rise of methane concentration first noted by the  
613 SAM instrument (Ls 336°) was at a transitional time at Gale Crater, when strong  
614 flushing northern winds that produce a wholesale inundation of the crater give way to  
615 less intense circulations typical of the rest of the year (PGR16). Based on the analysis  
616 of winds and potential temperature, PGR16 suggested that mixing between the crater air  
617 mass and the rest of the atmosphere was also reduced during the more quiescent times  
618 of year. The tracer studies provide a means to quantitatively test this hypothesis.

### 619 **3.1 Punctual methane release results**

620 In the punctual methane release scenarios, Ls 270° was shown to be, as  
621 expected, a faster mixing season when air within and outside the crater was well mixed  
622 by strong, flushing, northerly flow and large amplitude breaking mountain waves:  
623 downslope air driven both by buoyancy and dynamical forcing at night penetrates all the  
624 way down to the surface producing a wholesale inundation of the crater. In this punctual  
625 methane release inside of Gale crater scenario, the tracer #1 mixing ratio inside the  
626 crater is diluted to a few percent or less just 5 hours after the release both at Ls 90° and  
627 at Ls 270° (Figures 9 and 10). Also, if we take a look at log fraction (Figure 11) we can  
628 see how after 15 hours from the release (at 2000 Local Mean Solar Time, hereafter  
629 LMST), tracer #1 is diluted by five orders of magnitude from the initial concentration at  
630 Ls 90° and by eleven orders of magnitude at Ls 270°. Not only is tracer #1 removed  
631 quickly, but in that 15 hours period the fraction of external crater air (tracer #4) at the  
632 bottom of the crater replacing internal crater air is 80% at Ls 90° (when mixing is  
633 slightly more slower) and 100% at Ls 270° (when mixing is slightly more rapid). These  
634 results indicate that much of the air originates from outside the crater regardless of the  
635 season. Thus, the mixing of the crater air with the external environment is slightly

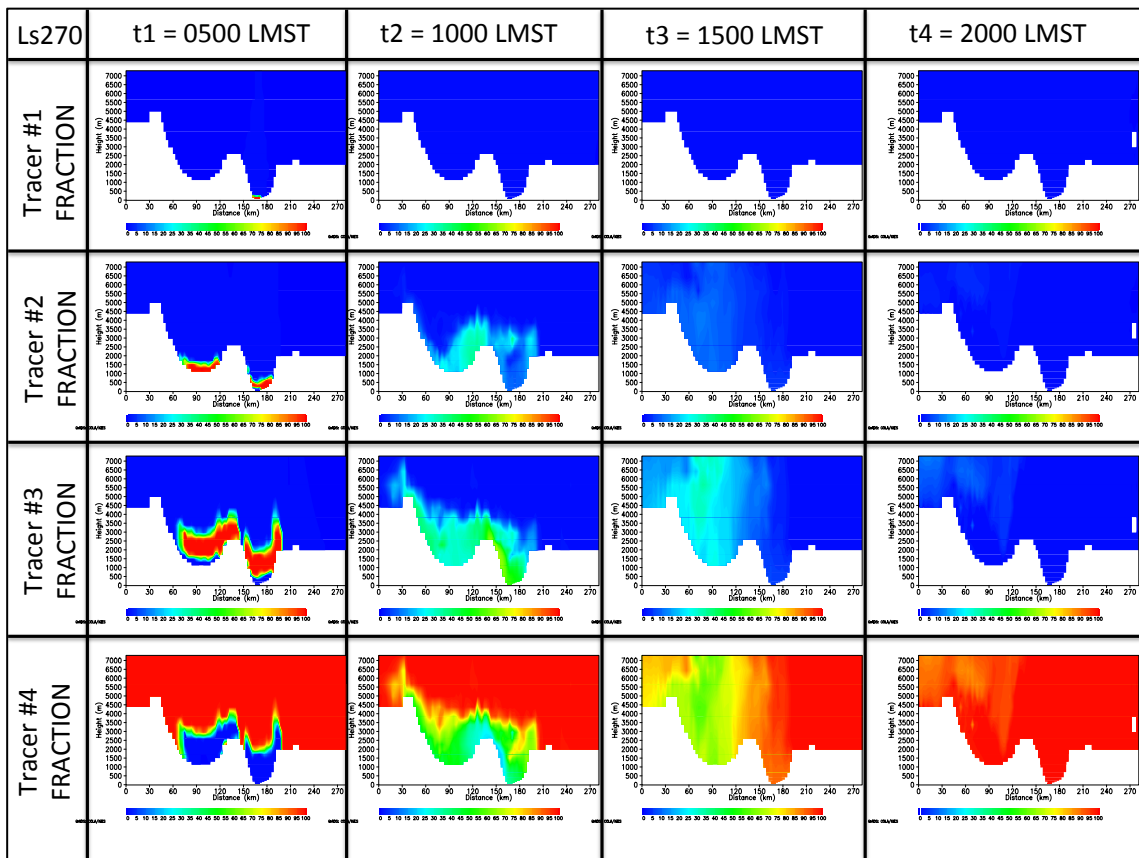
636 slower during the rest of the year compared to Ls 270° season, but the timescale it is  
 637 still rapid. Regardless of the season, the simulations indicate that the air mass of the  
 638 northern crater is evacuated and mixed away in one sol or less. These new results are  
 639 an important update to the 2016 work; the crater does not appear to be strongly isolated  
 640 at any time of year. Also, Ls 270° scenario reminds to a front passing where horizontal  
 641 incoming air mass from north hemisphere sweep the crater away (Figure 10 bottom,  
 642 Figure 11 bottom), while in the Ls 90° a much more vertical pattern is observed (Figure  
 643 9 bottom, Figure 11 up).



644

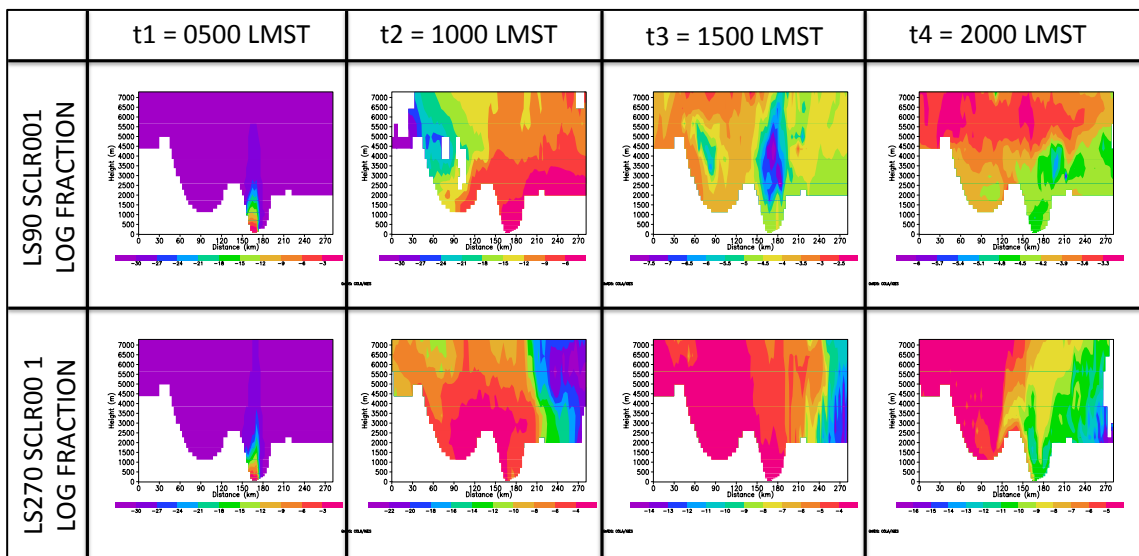
645 Figure 9. Fraction of the four tracers at four different times (0500, 1000, 1500 and 2000 LMST) at Ls  
 646 90° in a cross section view of the crater. E.g.  $\text{Fraction of tracer \#1} = \frac{\text{tracer \#1}}{\sum \text{tracer1+tracer2+tracer3+tracer4}}$





647

648 **Figure 10.** Same as Figure 9 but for Ls 270°

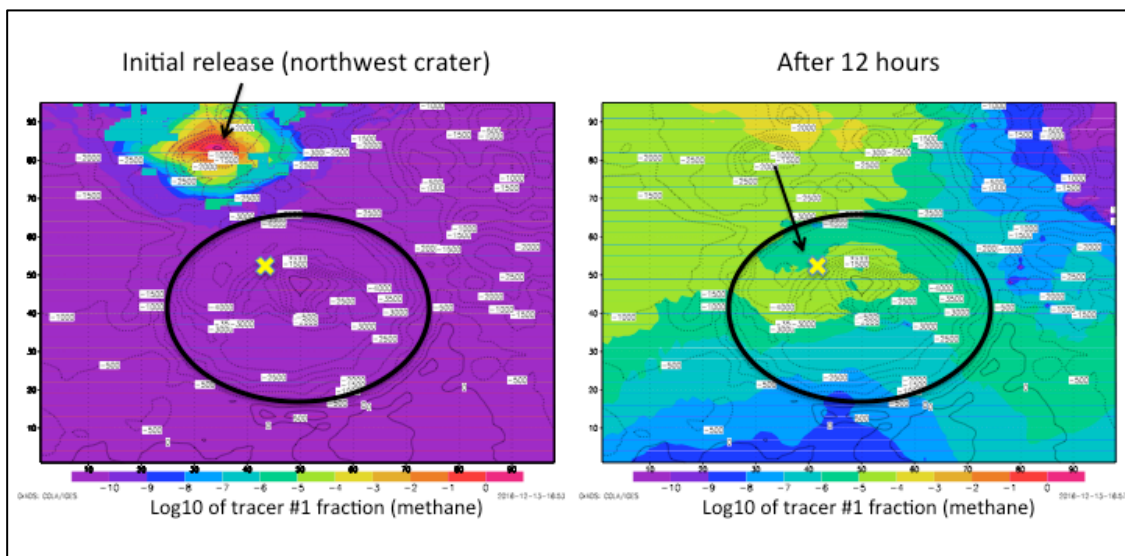


649

650 **Figure 11.** Same as Figure 9 and 10 but for log fraction at Ls 90° and Ls 270°

651 The punctual methane release scenario outside of Gale crater provides additional  
 652 insight into the potential transport of air into the crater. In this scenario, only 12 hours

653 after release, the methane that makes it to the MSL Curiosity rover location at ~14.5 m  
654 high (the lowest thermodynamic level where methane could be sampled in our  
655 simulations) is diluted by six orders of magnitude from the initial release concentration  
656 regardless of the season (Figure 12). Although the methane is transported towards the  
657 crater due to the northwesterly wind blowing towards the crater (as expected in  
658 PGR16), the methane is rapidly mixed vertically and horizontally. So, although the air  
659 in the crater is being rapidly replaced by outside air, there is a large amount of mixing  
660 and dispersion of the source air itself; it appears that a broad region of external air is  
661 mixed into the crater. To achieve a value of 1 ppbv at the rover location, an upwind  
662 release of methane on the order of parts per thousand would be required, which is likely  
663 unreasonable.



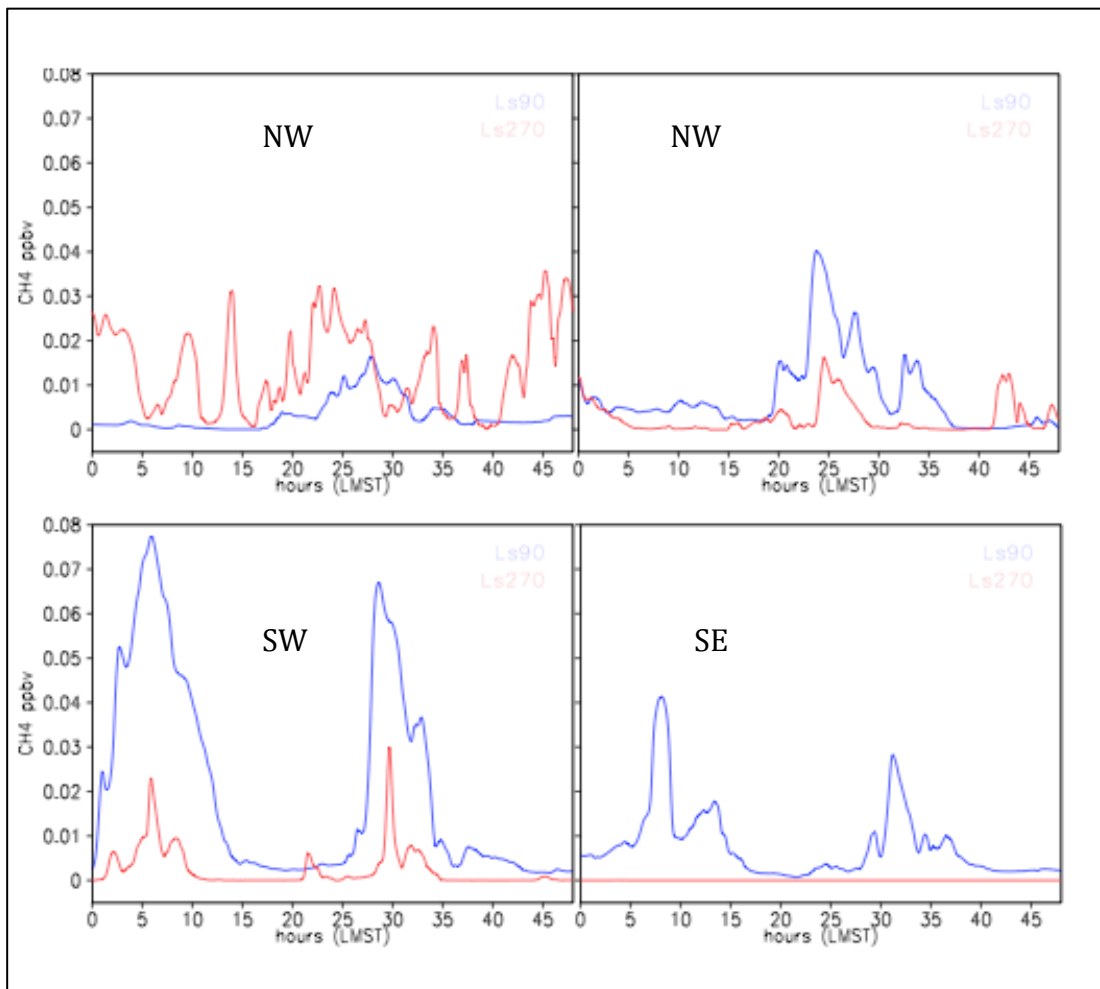
664

665 **Figure 12. Aerial view of tracer #1 (methane) fraction at ~14.5 m high with crater encircled at Ls 90°.**  
666 **Punctual methane released outside crater is diluted by approx. 6 orders of magnitude from the initial**  
667 **release concentration at rover location only 12 hours after emission regardless of the season. Same**  
668 **behavior is observed at Ls 270°..**

669

670 **3.2 Steady State methane release results**

671 In steady state methane release outside of Gale crater scenarios (NW, NE, SW and  
672 SE ~100 km outside crater), modeled abundances at the MSL Curiosity rover location  
673 are ~10 times lower (<0.08 ppbv) compared to SAM background levels (<0.7 ppbv) and  
674 ~100 times lower compared to the spikes (<8 ppbv) during all seasons both at Ls 90°  
675 and at Ls 270° and after being release from all locations outside of Gale crater (NW,  
676 NE, SW and SE) as can be shown in Figure 13. Each of the different releases are  
677 emitted and sampled independently. **When releasing from a source NW outside crater at**  
678 **Ls 270°, methane variations of one order of magnitude are sampled regardless of the**  
679 **time of the sol due to the strong flushing north component winds during all day (Figure**  
680 **13, upper left, red). In the other release locations experiments, the methane values are**  
681 **higher during nighttime, presumably because during night downslope winds from rims**  
682 **transport methane from release locations converging with Mt. Sharp downslope winds**  
683 **making methane contained at the very bottom of the crater, persisting and becoming**  
684 **trapped for longer inside Gale until daytime upslope winds sweep it away (Figure 13,**  
685 **except NW scenario).**



686

687 **Figure 13. Two sols timeseries of MRAMS methane abundances sampled at MSL location while being**  
 688 **released from steady state methane emission located outside of Gale crater (NW, NE, SW, SE). Each of**  
 689 **the different releases are emitted and sampled independently.**

690 In steady state methane release inside of Gale crater scenario (~1 grid point west  
 691 from the rover with an area of ~149 km<sup>2</sup>) when sampling the model at the source  
 692 location, methane values fluctuate from 0.1 to 1.2 ppbv (Figure 14). This is compatible  
 693 with SAM low background methane abundances and only ~6 times lower than the  
 694 methane spikes. **It is important to emphasize that these methane values are sampled at**  
 695 **~14.5 m high so a higher methane abundance is expected at ~1 m above release source**  
 696 **(using a five-parameter logistic -5PL- linear regression curve fitting method those peak**  
 697 **values at 1 m high are ~11 ppbv, and using a non-linear power regression curve fitting**  
 698 **method those peak values are ~4 ppbv).**

699 Thus, if the rover were directly over a release location, the SAM measurements  
700 could be consistent with a reasonable release associated with a flux similar to methane  
701 clathrate release.

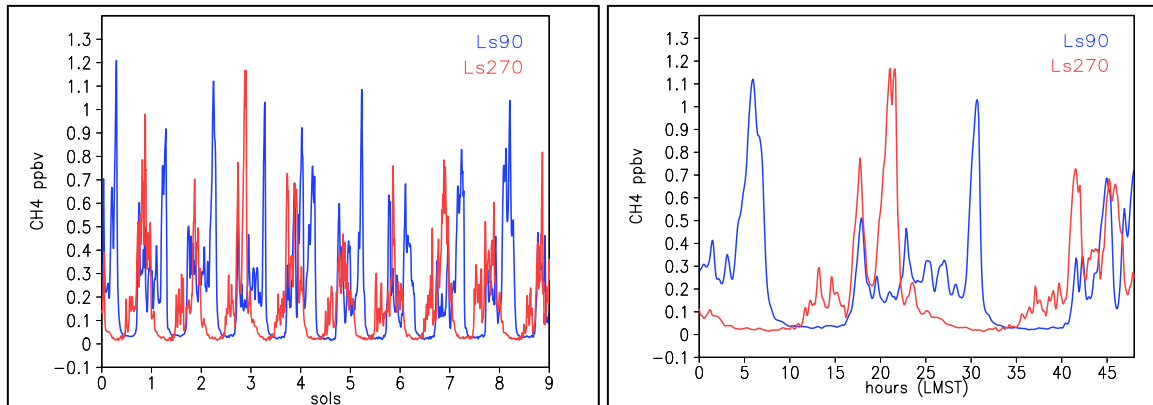


Figure 14. Nine sols timeseries (left) and two sols timeseries (right) of MRAMS methane abundances sampled at release location while being released from steady state methane emission located inside of Gale crater ~1 grid point west from the rover with an area of ~149 km<sup>2</sup>. Only nine of the twelve sols simulated were included into the figure).

702 Ls 155° is the highest methane values season in M09 (<45 ppbv) and also in  
703 MRAMS steady state methane release mimicking M09 scenarios when sampling at the  
704 rover location eleven sols after release at Ls 155° (~16 ppbv) compared to Ls 90° (~0.25  
705 ppbv) and Ls 270° (~0.8 ppbv) (Figure 15). This big difference could be due to Ls 155°  
706 is approaching to the spring equinoctial neutral global winds period (PGR16). Around  
707 the equinoxes, there is a brief transition period where the rising branch quickly crosses  
708 from one hemisphere into the other as it migrates to its more typical solstitial location.  
709 During this transition, there is convergence into the rising branch (similar to the  
710 intertropical convergence zone on Earth), and dual Hadley cells with one circulation in  
711 each hemisphere. Based on the mean meridional circulation, surface winds at the  
712 tropical location of Gale crater would be expected to go either way as the rising branch  
713 transits through the equatorial region containing and circulating methane rich air from  
714 M09 release areas in the intertropical zone. At solstices, those winds reverse with

715 northerly winds around Ls 270° and southerly winds around Ls 90° (PGR16) that could  
716 sweep methane rich air from M09 release areas away from equator.

717 As shown, even an area as large as the putative M09 release is insufficient to  
718 produce the amplitude of the sporadic higher spikes of methane measurable at MSL  
719 Curiosity rover during the SAM high spikes periods (~Ls 55-82°). At Ls 270° in these  
720 mimicking M09 scenarios, the methane values sampled at the rover location fluctuate  
721 from 0.1 to 0.8 ppbv. These values are compatible with SAM low background methane  
722 abundances and being only ~12 times lower than SAM direct ingest detections (high  
723 spikes).

724 When comparing the mimicking M09 full area (~8,000,000 km<sup>2</sup>) release  
725 scenario (Figure 15, bottom left) with the partial mimicking M09 area (~2,000,000 km<sup>2</sup>)  
726 release scenario (Figure 15, bottom right) both at Ls 270°, results show 30 times higher  
727 methane values with the larger release area, so the release size has also a large impact  
728 on the methane abundance sampled at the MSL Curiosity rover location.

729 The modeling results of steady state methane release mimicking M09 scenario at  
730 Ls 155° are in agreement with previous GCM modeling studies of methane plumes at  
731 the same season (Mischna et al. 2010; Karatekin et al. 2017; Viscardy et al. 2016)  
732 where the horizontal distribution of the methane cloud moves mainly in a east direction  
733 five sols after the surface release (Figure 16).

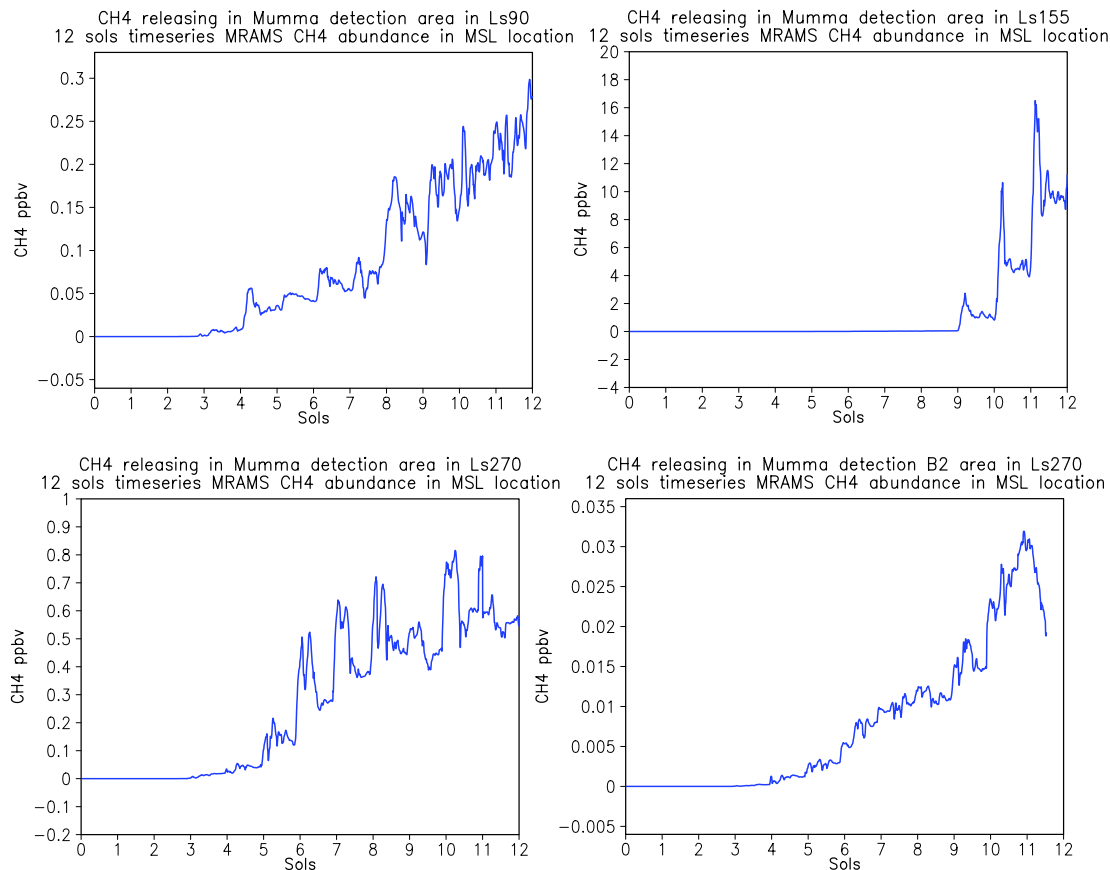
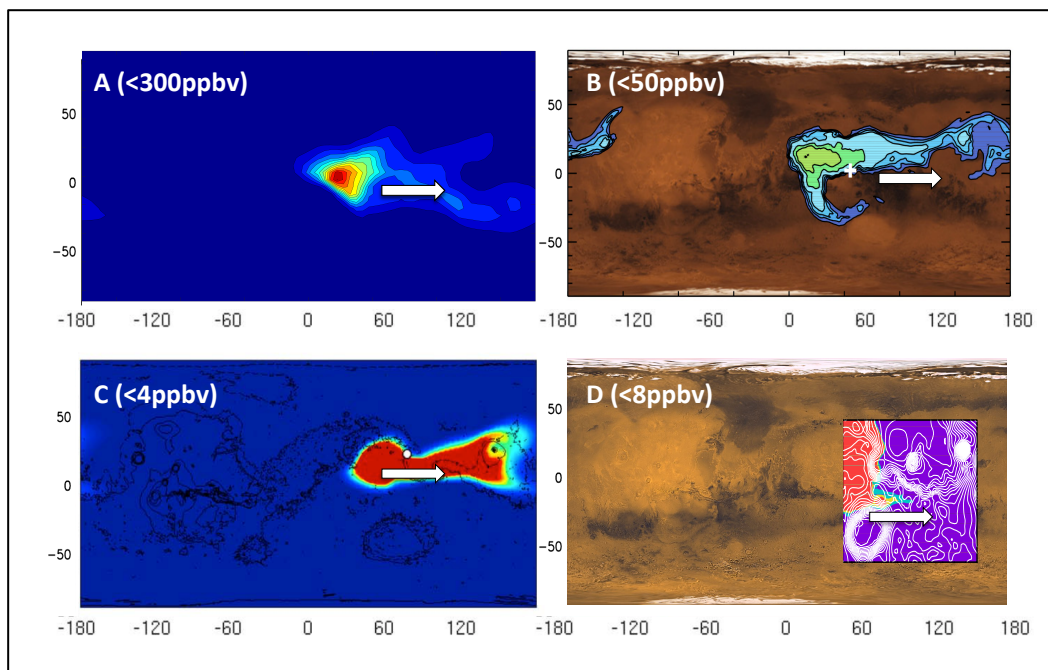


**Figure 15. Twelve sols timeseries of MRAMS methane abundances sampled at release location while being released from steady state methane emission located inside of Gale crater ~1 grid point west from the rover with an area of ~149 km<sup>2</sup>**



734

735  
736  
737  
738

**Figure 16. Horizontal distribution of methane mixing ratio (in ppbv) 5 sols after surface release of methane in M09 release area at Ls = 155°. Karatekin et al. 2017 (A; GCM), Mischna et al. 2011 (B; GCM), Viscardy et al. 2016 (C; GCM), Pla-García et al. 2018 (D, this paper results with mesoscale model) shows the same easterly pattern of the methane plume five sols after the release.**

739 Also our simulations show that surface emissions of methane results in a non-uniform  
740 vertical distribution (~5-20 kms), including the formation of elevated layers five sols  
741 after the release (supplementary material), that is in agreement with Viscardy et al.  
742 2016.

#### 743 **4 Discussion**

744 The Mars Regional Atmospheric Modeling System (MRAMS), used to study the  
745 transport and mixing of methane from specified source locations using tracers, help us  
746 to investigate whether methane releases, punctual or steady state, inside or outside of  
747 Gale crater, during summer time or the rest of the year, are consistent with SAM  
748 observations.

749 The punctual release scenarios indicate that the timescales of mixing in the crater is  
750 ~1 sol during all seasons, which is much faster than previously estimated. For there to  
751 be an extended period (> 1 sol) of enhanced methane abundance in the crater, there  
752 must be either a nearby steady release to counteract atmospheric mixing or there must  
753 be an extensive and highly enriched methane air mass; however, this would contradict  
754 the Mischna et al. 2011 modeling study indicating a single rather than extended period  
755 of release. Further, an extended, large release would result in average global values in  
756 excess of the background SAM value after mixing, unless the unknown rapid  
757 destruction mechanism is invoked, like the ones described in the introduction section  
758 (dust electrochemistry and wind eroding surface quartz grains).

759 For the elevated methane levels in the crater to drop rapidly back to background  
760 levels, at least two things would need to happen. First, the external crater environment  
761 would have to drop at least as rapidly to the background levels. This seems possible



762 only if there is very deep mixing that spreads the release through a very large volume of  
763 atmosphere, or if a rapid destruction mechanism is invoked. The second thing that  
764 would have to happen is that the crater air would have to mix nearly completely with  
765 the external crater air. Although mixing seems slightly slower the rest of the year other  
766 than Ls 270°, it may still be possible that the mixing time scale is sufficient to affect the  
767 necessary change as shown in our punctual methane release scenarios (Figures 9 and  
768 11).

769         The timing of SAM sample ingestion is very important looking at the steady  
770 state methane release inside Gale crater scenario results because they show diurnal  
771 methane variations of one order of magnitude, increasing during the evening and night,  
772 and decreasing during the daytime (Figure 13 –except NW at 270°- and Figure 14).  
773 Again, most of the SAM-TLS measurements were acquired during nighttime (except on  
774 sols 305 and 525) due to thermal requirements of the SAM sample handling system, but  
775 we do not have the exactly acquisition times so we can not study the influence of the  
776 local ingestion time into the measurements. During daytime, upslope winds through the  
777 crater rims and Mt. Sharp could sweep the air out of the crater dragging methane with  
778 them (Figure 17 upper left, 1300 LMST), and during nighttime the process reverse with  
779 downslope winds from rims and Mt. Sharp that converge and contain methane at the  
780 very bottom of the crater, persisting and becoming trapped for longer close to the point  
781 where it is released (Figure 17, 1900 LMST, 0100 LMST and moreover 0700 LMST).  
782 This behavior emphasize the importance of the horizontal mixing. Horizontal and not  
783 only vertical mixing should be taken into account when studying atmospheric methane  
784 circulation. Also and as previously mentioned, gases released in the crater could  
785 become trapped in the lowest portion of the crater basin due to the very cold and dense

786 air mass that would be resistant to mixing with air above helping to the converging  
 787 downslope winds to contain methane close to the release area.

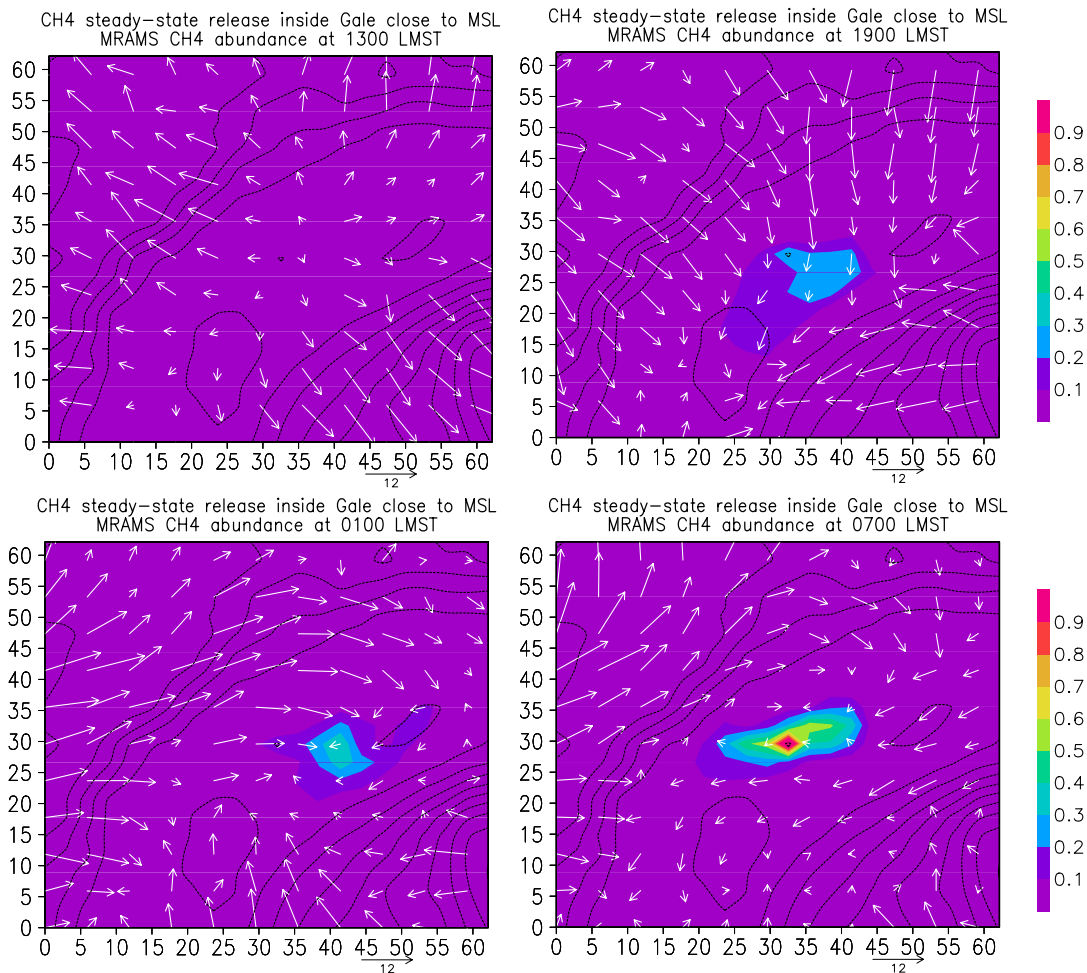


**Figure 17. Areal view of methane mixing ratio for a steady state methane release close ~1 grid point west from the rover location. During nighttime the downslope winds from rims and Mt. Sharp converge and contain methane at the very bottom of the crater, persisting and becoming trapped for longer close to the point where it is released**

788

789 Based on global circulation modeling, methane could also be subject during  
 790 daytime to turbulent convective vertical mixing in the planetary boundary layer  
 791 (hereafter PBL) and mixed upward rapidly to the top of this atmospheric layer  
 792 (Viscardy et al. 2016). When the PBL decreased (and therefore also turbulent  
 793 convective vertical mixing) in the late afternoon, followed by the development of

794 nocturnal inversion after sunset, it could help to the mentioned converging downslope  
795 winds (both from rims and Mt. Sharp) to contain the methane close to release location.

796 As discussed in PGR16 and further confirmed with this article results, the  
797 circulation in and around Gale Crater is extremely complex and varies seasonally. The  
798 circulation is strongly 3-D, not just 1-D or 2-D, and any scenario describing the  
799 transport of methane must recognize this dimensionality. The source location of  
800 methane emission cannot be determined by simply looking upstream and variations of  
801 methane concentration cannot be determined by simply considering 1-D vertical mixing  
802 based on PBL height. Further, because of the complexity of the circulation, the local  
803 wind at the rover location may not be representative of the larger prevailing wind.  
804 Consequently, trying to determine the source location of methane based on REMS wind  
805 estimates at the time of the SAM measurements or trying to explain a putative  
806 suppressed mixing with a PBL suppression is a dubious proposition.

807 The only plausible scenario to reconcile observations and the modeling results is an  
808 intermittent local steady state release very close to the rover with the additional  
809 restriction that such releases must be globally rare (in other words claiming that Gale  
810 crater is a unique place on Mars, on the other hand something highly unlikely) or there  
811 must be a unknown rapid methane destruction mechanism that prevent from a rapid  
812 increase of the background methane level that would be detected by SAM.

813 Although being so lucky to have the rover moving just above a methane release  
814 location and having methane spikes lasting just a sol or some sols are extraordinary  
815 claims, we can explain them and are compatible with our modeling results. But, if the  
816 spike lasted for a long time, similar to the period without SAM measurements between

817 spikes (that is ~200 sols), it becomes much difficult to interpret. While Gale crater may  
818 be a special place, it almost certainly is not unique. If methane is being released locally  
819 in the crater, it should also be released elsewhere on Mars. Thus, a release of long  
820 duration at Gale crater would also happen elsewhere, and this would have result in a  
821 background global methane abundance above that measured by SAM, again assuming  
822 no rapid and efficient destruction mechanisms.

#### 823 **4.1 A possible explanation to the methane background seasonal cycle**

824 The MSL-SAM team recently presented in situ measurements of the background  
825 methane levels in Gale Crater that exhibits a strong, repeatable seasonal variability  
826 ranging from about 0.3 ppbv to about 0.7 ppbv with a mean value of ~0.4 ppbv over  
827 more than two martian years (Webster et al. 2017). The observed large seasonal  
828 variation in the background and sporadic observations of higher pulses of ~7 ppbv  
829 appear consistent with localized small sources of methane releases from Martian surface  
830 reservoirs that may be occurring throughout the planet.

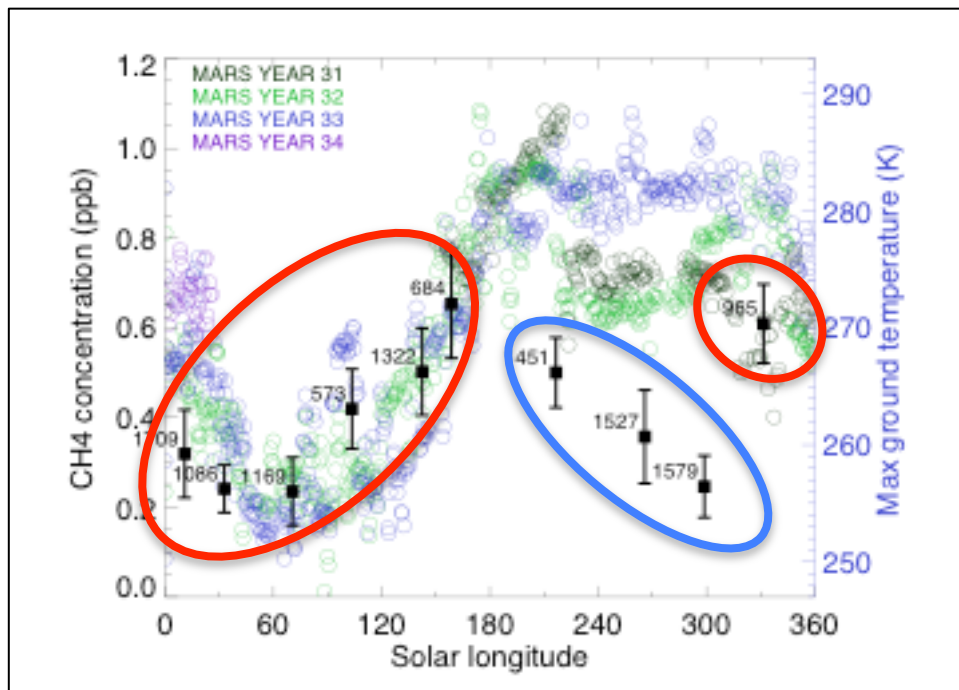
831 The origin of methane variability is an active area of research, and our  
832 colleagues on the MSL team (John E. Moores and co-authors) are working to better  
833 model adsorption on and diffusion through the regolith, as well as the impact of the  
834 depth of the boundary layer on vertical mixing. Because PBL is especially suppressed at  
835 Gale crater (Newman et al. 2017; PGR16; Moores et al. 2015), then vertical mixing is  
836 very limited too. It has been proposed that this vertical mixing limitation makes Gale  
837 crater a very special place, because methane would persist for longer close to the point  
838 where it is emitted and background concentrations observed should be substantially  
839 higher compared to other locations on Mars. But there is a major flaw on this theory,  
840 which is that it really only considers vertical mixing. Even a highly stratified boundary

841 layer with limited vertical mixing could be flushed out with strong horizontal winds  
842 flowing into and out of the crater. The influence of the height of the PBL could be  
843 important, or it could be mostly irrelevant. But again, and as previously mentioned,  
844 what we found in our simulations is that mixing is high during all the martian year,  
845 being slightly more rapid at Ls 270° compared to other seasons when there is still quite  
846 mixing, so crater is not isolated in any period of the year and any gas inside the crater is  
847 diluted and diffused away regardless of the season. As previously noted, horizontal and  
848 not only vertical mixing should be taken into account. PBL could be very suppressed  
849 and therefore vertical mixing too while having a strong horizontal mixing. Again, the  
850 circulation is strongly 3-D, not just 1-D or 2-D, and any scenario describing the  
851 transport of methane must recognize this dimensionality.

852         It could be an alternative explanation, other than PBL high variation during  
853 Mars year for the seasonal background methane cycle. Presumably, ground temperature  
854 controls the release of methane trapped in clathrates on seasonal timescales. The  
855 methane flux should be higher during warmer seasons, implying a seasonal hemispheric  
856 difference in methane background values if we assume ubiquitous release sources over  
857 the planet, with higher values in the summer hemisphere and lower in the winter  
858 hemisphere. The origin of the external air could be very different depending on the  
859 season (PGR16). For example, during Ls 225-315°, the strong northwesterly air  
860 flowing down the crater rims during nighttime and easily making it to the crater floor  
861 originates from deep within the northern hemisphere, whereas at other seasons the  
862 origin of that external air is from locations closer to the crater or from more tropical  
863 regions. This matters because if ground temperature is controlling emission, different  
864 locations and hemispheres will emit differently at different seasons.

865           Maximum emission at Gale crater would correspond with minimum emission in  
866 the north hemisphere and vice versa. The consequence of this is that although the local  
867 methane emission in the crater may be highest during the warm Ls 225-315° season,  
868 those emissions are rapidly transported and swept away and replaced by methane poor  
869 air emanating from the cold northern hemisphere. So, even with a maximum emission at  
870 Gale, the methane background levels inside crater should be poorly correlated with  
871 ground temperature at Ls 225-315° (Figure 18, blue circles) due to the methane rich  
872 internal crater air from local releases is being rapidly replaced/mixed by/with a  
873 wholesale inundation of methane poor external crater air from the north hemisphere  
874 with a lower background level (in the north hemisphere release areas there should be  
875 less chances to stress the rock to create cracks or to thin ice barriers due to be cooler),  
876 something shown from Ls 216° -sol 1451- to Ls 298° -sol 1579- in Figure 18.

877           In contrast, the methane flux in the crater at other seasons is similar to the flux  
878 for the source air location. In this scenario, mixing has little effect on the overall  
879 methane concentration and the concentration should be better correlated with the local  
880 ground temperature. During the colder seasons, enrichment observations have  
881 reasonable good correlation with ground temperatures from Ls 331° -sol 965- to Ls 158°  
882 -sol 684- (Figure 18, red circles) when the methane poor internal crater air is mixed  
883 with methane poor external crater air from south hemisphere.



884  
885  
886  
887  
888  
889

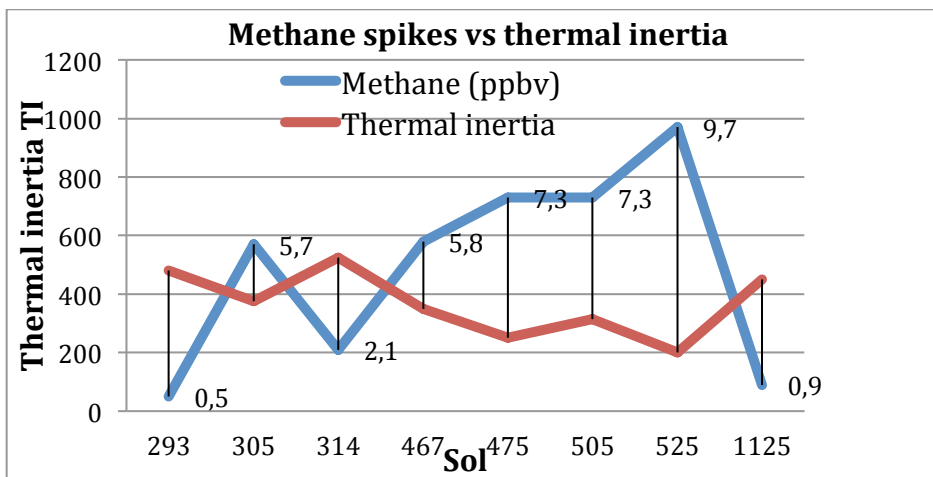
Figure 18. Background methane [enrichment] measurements (black squares with sol numbers) compared with maximum ground temperature (colored circles). Correlation is better in southern late summer/fall/winter (Ls 331-158°) than in southern late spring/early summer (Ls 216-298°) because background methane values from putative local releases (encircled in red) are not so well mixed with external crater air masses as the other ones (encircled in blue). Adapted from Webster et al. 2018

890  
891  
892  
893  
894  
895  
896  
897  
898  
899  
900  
901

#### 4.2 Impact of the thermal inertia into the methane spikes

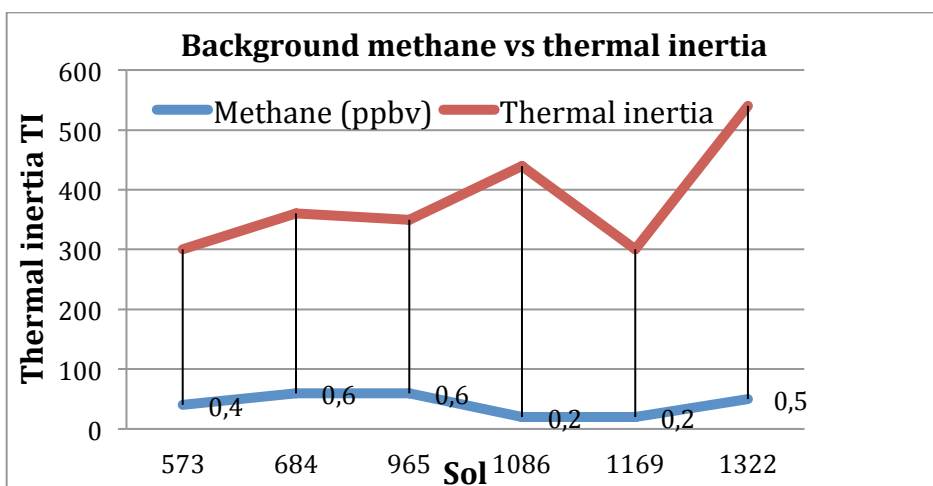
To determine the global clathrate stability zones map (Figure 5) and the methane flux described in section 2.2, KG17 used the thermal inertia derived by TES MGS observations, with a surface mean thermal inertia for Gale crater of 365. The recent results from Vasavada et al. 2017 shows a much lower thermal inertia in Gale crater, ranging from 200 to 350 TI depending on the type of soil inside the crater. The surface methane flux for a given source depth and a given amount of methane should be higher with lower thermal inertia (Elodie Gloesener personal communication). The diffusion coefficient depends on the temperature and the methane flux should be larger when temperature is more important (so when thermal conductivity and thermal inertia are lower). Indeed in the KG17 simulations, the surface flux is 13% larger for TI = 200 compared to TI = 500.

902 Although correlation does not imply causation, the good agreement of methane  
 903 spikes sols with very low thermal inertia Gale crater soils (Table 4) is at least curious.  
 904 Maybe putative local clathrates releases could be producing methane spikes when soils  
 905 conditions are appropriate. This behavior is not observed in the background methane  
 906 enrichment measurements sols (Table 5). So assuming the same clathrate reservoirs and  
 907 the same dependence with seasons both for spikes and background level sols, maybe the  
 908 thermal inertia is making the difference.



909

Table 4. Thermal inertia values vs TLS-SAM direct ingest sols methane values



911

Table 5. Thermal inertia values vs TLS-SAM enrichment detections

912



## 913 **5 Conclusion**

914 The MRAMS model is well suited to study evolution, transport and mixing of methane  
915 from potential source locations using tracers. Clathrate hydrates could be a possible  
916 source of episodic methane releases on Mars, and are used to estimate atmospheric  
917 abundances based on reasonable surface flux rates.

918 For a small short (punctual in time) methane release inside Gale crater, we find that  
919 all methane is gone within 5 hours regardless of season. Although the mixing time is  
920 somewhat longer for seasons outside of Ls 270°, mixing is generally rapid. The  
921 hypothesis of a partially isolated crater in PGR16 is not supported by the tracer studies.  
922 For a limited area short methane release NW outside Gale crater, methane is diluted by  
923 6 orders of magnitude in similar time. In both cases regardless of the season. Indeed,  
924 timescales of mixing are ~1 sol, much faster than previously thought in PGR16.  
925 Duration of methane peak observed by SAM is ~100 sols (assuming no high frequency  
926 variations), so there must be a steady state release to counteract atmospheric mixing.  
927 This is in contrast with Mischna et al. 2011 work, where M09 observations can be  
928 reproduced best if the release is nearly punctual rather than a slow, steady emission.

929 In the steady state release scenarios (mimicking expectations for clathrate  
930 releases) MRAMS shows daily variations of an order of magnitude and this can impact  
931 the observed methane levels, so that timing of TLS-SAM measurements is very  
932 important.

933 It is very difficult to explain the SAM measurements using global scale  
934 photochemical models with global transport. But, the circulations in Gale Crater are  
935 extremely complex and local meteorology plays a major role.

936 In the steady state release outside (NW, NE, SW and SE) Gale scenarios, the  
937 nighttime downslope flows through crater rims pushes methane from the external  
938 release areas inside the crater. Only with a source release NW outside crater we sample  
939 methane spikes with MRAMS during daytime due to the strong flushing north  
940 component winds.

941 In the steady state methane release inside Gale crater scenario, methane  
942 increases during the evening and night, and decreases during the daytime (Figure 14).  
943 During daytime, upslope winds through the crater rims and Mt. Sharp could sweep the  
944 air out of the crater dragging methane with them, and during nighttime the process  
945 reverse with downslope winds from rims and Mt. Sharp that converge and contain  
946 methane at the very bottom of the crater, persisting and becoming trapped for longer  
947 close to the point where it is released. Also and as previously mentioned, gases released  
948 in the crater could become trapped in the lowest portion of the crater basin due to the  
949 very cold and dense air mass that would be resistant to mixing with air above helping to  
950 the converging downslope winds to contain methane close to the release area.

951 Ls 155° is the highest methane values season in M09 (<45 ppbv) and also in  
952 MRAMS steady state methane release mimicking M09 scenarios when sampling at the  
953 rover location eleven sols after release at Ls 155° (~16 ppbv). Based on the mean  
954 meridional circulation, surface winds at the tropical location of Gale crater would be  
955 expected to go either way as the rising branch transits through the equatorial region  
956 containing and circulating methane rich air from M09 release areas in the intertropical  
957 zone where Gale crater is. These are the highest methane values (~16 ppbv) sampled at  
958 the rover location in all our experiments, but are incompatible with the periods when  
959 SAM detected the methane spikes.

960           The atmospheric circulation at Gale crater is strongly 3-D, not just 1-D or 2-D,  
961 and any scenario describing the transport of methane must recognize this  
962 dimensionality. The variations of methane concentration cannot be determined by  
963 simply looking upstream, or by simply considering 1-D vertical mixing based on PBL  
964 height. Further, because of the complexity of the circulation, the local wind at the rover  
965 location may not be representative of the larger prevailing wind. Consequently, trying  
966 to determine the source location of methane based on REMS wind estimates at the time  
967 of the SAM measurements or trying to explain a putative suppressed mixing with a PBL  
968 suppression is a dubious proposition.

969           It is difficult to reconcile the SAM peak methane detections with the atmospheric  
970 transport and mixing predicted by MRAMS **in the same periods** with our initial  
971 conditions (KG17 fluxes rates, release areas sizes and distances to MSL Curiosity  
972 rover). The only plausible scenario is an intermittent local steady state release close to  
973 the rover with the additional restriction that such release must be globally rare (this is  
974 highly unlikely because Gale crater is not a unique place on Mars) or there must be an  
975 unknown rapid methane destruction mechanism. Even if it were possible, what are the  
976 chances that the rover Curiosity would be so lucky as to operate just above the source or  
977 nearby the source as it moved?

978           If we multiply flux, increase release area or move it closer to rover (or all of  
979 previous), it could be possible to get sporadic higher spikes (~7.2 ppbv) of methane that  
980 SAM should be capable to detect regardless where it comes from: inside Gale, outside  
981 (close to) Gale or far away from Gale. Of course, there are physical and reasonable  
982 limits to the size and magnitude of a methane release. As shown, even an area as large

983 as the putative M09 release is insufficient to produce these sporadic higher spikes of  
984 methane measurable at the rover location. It is also challenging to imagine an emission  
985 rate that is one to two orders of magnitude larger than KG17.

986 Due to the high mixing rate reported in our results, it is quite possible that the value  
987 could decay to the background levels after spikes in the given time. Thus, from a mixing  
988 standpoint, these scenarios seems at least plausible, however they require a form of  
989 special pleading. There is nothing exceptionally special about Gale Crater. It is hard to  
990 argue that if methane is being released on Mars, that Gale Crater is the sole source.  
991 Rather, if it is coming out at Gale Crater, it is likely to be coming out in many other  
992 places on Mars. If that is the case, then the background values should likely be far  
993 higher than the observed values.

994 Some new hypotheses are proposed trying to explain the seasonal cycle of  
995 methane background levels and the methane spikes. For the seasonal cycle of methane  
996 background, maybe the ground temperature controls the release of methane trapped in  
997 clathrates on seasonal timescales with a higher methane flux during warmer seasons,  
998 implying a hemispheric difference in methane background values assuming an  
999 ubiquitous release sources over the planet. Then the poor correlation of ground  
1000 temperature with methane background level (low values in the warmer periods) during  
1001 Ls 216-298° could be explained due to a wholesale inundation of methane poor external  
1002 crater air from the north hemisphere that rapidly replace/mix by/with methane rich  
1003 internal crater air from local releases. For the methane spikes, maybe putative local  
1004 releases could be producing them when soils conditions (very low thermal inertia) are  
1005 appropriate.

1006 The instrument NOMAD (Nadir and Occultation for MArS Discovery) a  
1007 spectrometer suite on board ESA ExoMars Trace Gas Orbiter (TGO) will provide from  
1008 next May 2018 the spectrum of sunlight across a wide range of wavelengths, enabling  
1009 the valuable detection of the volatile reservoirs on Mars atmosphere and particularly the  
1010 sources and the sinks of methane (it is designed to measure the first vertical profiles of  
1011 methane on Mars) and other important trace gases, providing insights into the nature of  
1012 their sources through the study of gas ratios and isotopes, even in low concentrations,  
1013 with high sensitivity up to a thousand times more resolution than its predecessors. In  
1014 addition to identifying the constituents of the Martian atmosphere, NOMAD will also  
1015 map their locations. These future TGO observations will help to validate our MRAMS  
1016 methane simulations.

## 1017 **6 Acknowledgements**

1018 As with all large space missions, the ability to conduct science depends upon the  
1019 dedication of hundreds of scientists, engineers and managers. The authors are grateful  
1020 for the hard work of the MSL team, without whose dedication none of this work could  
1021 be accomplished. The authors would also like to explicitly thank the MSL science team  
1022 for their efforts. Additionally, this manuscript benefited greatly from comments and  
1023 discussions provided by Scot C. R. Rafkin (Southwest Research Institute), Özgür  
1024 Karatekin (Royal Observatory of Belgium), Elodie Gloesener (Royal Observatory of  
1025 Belgium), Alberto G. Fairén (Cornell/Centro de Astrobiología), Timothy Michaels  
1026 (SETI), Lorie Bruhwiler (NOAA), Cesar Menor-Salván (Georgia Tech), Christopher R.  
1027 Webster (NASA Jet Propulsion Laboratory), John E. Moores (Centre for Research in  
1028 Earth and Space Science, CRESS) and Paul R. Mahaffy (NASA Goddard Space Flight  
1029 Center). This work was supported by the NASA/Jet Propulsion Laboratory under

1030 subcontract 1356597 and by the Spanish Ministry of Economy and Competitiveness  
1031 under contracts MINECO ESO2016-79612-C3-1-R. Part of this research was carried  
1032 out at the Jet Propulsion Laboratory, California Institute of Technology, under a  
1033 contract with the National Aeronautics and Space Administration.

## 1034 **7 Supplementary material**

1035 Supplementary material associated with this article can be found, in the online  
1036 version, at:

1037 <https://data.boulder.swri.edu/jpla/CH4paperSupplementaryMaterial/>

## 1038 **8 References**

1039 Aoki, S. et al. (2018, September). Search of CH<sub>4</sub> on Mars using EXES aboard  
1040 SOFIA. In “From Mars Express to ExoMars” Workshop (27–28 February 2018, ESAC  
1041 Madrid, Spain).

1042 Aoki, S. et al. (2017, September). Sensitive search of CH<sub>4</sub> on Mars by  
1043 SOFIA/EXES. In European Planetary Science Congress (Vol. 11).

1044 Atreya, S. K., Mahaffy, P. R., & Wong, A. S. (2007). Methane and related trace  
1045 species on Mars: Origin, loss, implications for life, and habitability. *Planetary and*  
1046 *Space Science*, 55(3), 358-369.

1047 Conrath, B. J. (1975). Thermal structure of the Martian atmosphere during the  
1048 dissipation of the dust storm of 1971. *Icarus*, 24(1), 36-46.

1049 Chastain, B. K., & Chevrier, V. (2007). Methane clathrate hydrates as a potential  
1050 source for martian atmospheric methane. *Planetary and Space Science*, 55(10), 1246-  
1051 1256.

1052           Encrenaz, T. (2008). Search for methane on Mars: Observations, interpretation  
1053 and future work. *Advances in Space Research*, 42(1), 1-5.

1054           Etiope, G., Oehler, D. Z., & Allen, C. C. (2011). Methane emissions from  
1055 Earth's degassing: Implications for Mars. *Planetary and Space Science*, 59(2), 182-  
1056 195.

1057           Fonti, S. E. R. G. I. O., & Marzo, G. A. (2010). Mapping the methane on Mars.  
1058 *Astronomy & Astrophysics*, 512, A51.

1059           Formisano, V., Atreya, S., Encrenaz, T., Ignatiev, N., & Giuranna, M. (2004).  
1060 Detection of methane in the atmosphere of Mars. *Science*, 306(5702), 1758-1761.

1061           Geminale, A., Formisano, V., & Sindoni, G. (2011). Mapping methane in  
1062 Martian atmosphere with PFS-MEX data. *Planetary and Space Science*, 59(2), 137-  
1063 148.

1064           Geminale, A., Formisano, V., & Giuranna, M. (2008). Methane in Martian  
1065 atmosphere: average spatial, diurnal, and seasonal behaviour. *Planetary and Space*  
1066 *Science*, 56(9), 1194-1203.

1067           Gloesener, E., Karatekin, O., & Dehant, V. (2017, January). CH<sub>4</sub>-rich  
1068 Clathrate Hydrate Stability Zone in the present Martian Subsurface. In *The Sixth*  
1069 *International Workshop on the Mars Atmosphere: Modelling and observation* (p.  
1070 4209).

1071           Gomez-Elvira, J., et al. (2012). "REMS: The environmental sensor suite for  
1072 the Mars Science Laboratory rover", *Space Sci. Rev.*, 170, 583-640,  
1073 doi:10.1007/s11214-012-9921-1.

1074 Holmes, J. A., Lewis, S. R., & Patel, M. R. (2015). Analysing the consistency of  
1075 martian methane observations by investigation of global methane transport.  
1076 *Icarus*, 257, 23-32.

1077 Kahre, M. A., J. R. Murphy and R. M. Haberle (2006). Modelling the Martian  
1078 dust cycle and surface dust reservoirs with the NASA Ames general circulation  
1079 model. *Journal of Geophysical Research E: Planets* 111(6).

1080 Karatekin, Ö., Gloesener, E., & Temel, O. (2017, April). Clathrate hydrates as  
1081 possible source of episodic methane releases on Mars. In EGU General Assembly  
1082 Conference Abstracts (Vol. 19, p. 11000).

1083 Karatekin, O., Gloesener, E., Dehant, V. M. A., & Temel, O. (2016, February).  
1084 Methane clathrate stability zone variations and gas transport in the Martian  
1085 subsurface. In AGU 2016 Fall Meeting Abstracts. P21B2088K

1086 Keppler, F., Vigano, I., McLeod, A., Ott, U., Früchtl, M., & Röckmann, T.  
1087 (2012). Ultraviolet-radiation-induced methane emissions from meteorites and the  
1088 Martian atmosphere. *Nature*, 486(7401), 93-96.

1089 Krasnopolsky, V. A. (2012). Search for methane and upper limits to ethane  
1090 and SO<sub>2</sub> on Mars. *Icarus*, 217(1), 144-152.

1091 Krasnopolsky, V. A. (2011, October). A sensitive search for methane and  
1092 ethane on Mars. In EPSC-DPS Joint Meeting 2011 (p. 49).

1093 Krasnopolsky, V. A. (2007). Long-term spectroscopic observations of Mars  
1094 using IRTF/CSHELL: Mapping of O<sub>2</sub> dayglow, CO, and search for CH<sub>4</sub>. *Icarus*,  
1095 190(1), 93-102.

1096 Krasnopolsky, V. A., Maillard, J. P., & Owen, T. C. (2004). Detection of  
1097 methane in the martian atmosphere: evidence for life?. *Icarus*, 172(2), 537-547.



1098 Lefevre, F., & Forget, F. (2009). Observed variations of methane on Mars  
1099 unexplained by known atmospheric chemistry and physics. *Nature*, 460(7256),  
1100 720-723.

1101 Malek, E., Davis, T., Martin, R.S. and Silva, P.J., 2006. Meteorological and  
1102 environmental aspects of one of the worst national air pollution episodes (January,  
1103 2004) in Logan, Cache Valley, Utah, USA. *Atmospheric research*, 79(2), pp.108-122.

1104 McMahon, S., Parnell, J., & Blamey, N. J. (2013). Sampling methane in basalt  
1105 on Earth and Mars. *International Journal of Astrobiology*, 12(2), 113-122.G.

1106 Meslin, P. Y., Gough, R., Lefèvre, F., & Forget, F. (2011). Little variability of  
1107 methane on Mars induced by adsorption in the regolith. *Planetary and Space*  
1108 *Science*, 59(2), 247-258.R. V. Gough, M. A. Tolbert, C. P. McKay, O. B. Toon, *Icarus*  
1109 207, 165–174 (2010).

1110 Mischna, M. A., Allen, M., Richardson, M. I., Newman, C. E., & Toigo, A. D.  
1111 (2011). Atmospheric modeling of Mars methane surface releases. *Planetary and*  
1112 *Space Science*, 59(2), 227-237.

1113 Moores, J. E., Smith, C. L., & Schuerger, A. C. (2017). UV production of  
1114 methane from surface and sedimenting IDPs on Mars in light of REMS data and  
1115 with insights for TGO. *Planetary and Space Science*, 147, 48-60.

1116 Moores, J. E., Lemmon, M. T., Kahanpää, H., Rafkin, S. C., Francis, R., Pla-  
1117 Garcia, J., ... & Vasavada, A. R. (2015). Observational evidence of a suppressed  
1118 planetary boundary layer in northern Gale Crater, Mars as seen by the Navcam  
1119 instrument onboard the Mars Science Laboratory rover. *Icarus*, 249, 129-142.

1120 Mumma, M. J. et al. (2009). Strong release of methane on Mars in northern  
1121 summer 2003. *Science*, 323(5917), 1041-1045.

1122 Newman, C. E. et al. (2017). Winds measured by the Rover Environmental  
1123 Monitoring Station (REMS) during the Mars Science Laboratory (MSL) rover's  
1124 Bagnold Dunes Campaign and comparison with numerical modeling using  
1125 MarsWRF. *Icarus*, 291, 203-231.

1126 Oze, C., & Sharma, M. (2005). Have olivine, will gas: Serpentinization and  
1127 the abiogenic production of methane on Mars. *Geophysical Research Letters*,  
1128 32(10).

1129 Pielke, R. A. et al. (1992). "A comprehensive meteorological modeling  
1130 system—RAMS." *Meteorology and Atmospheric Physics* 49(1): 69-91.

1131 Pla-Garcia, J. (2017) "El enigma del metano en Marte". *Astronomia Journal*,  
1132 219, 14

1133 Pla-Garcia, J. et al. (2016). The meteorology of Gale crater as determined  
1134 from rover environmental monitoring station observations and numerical  
1135 modeling. Part I: Comparison of model simulations with observations. *Icarus*, 280,  
1136 103-113.

1137 Poch, O., Kaci, S., Stalport, F., Szopa, C., & Coll, P. (2014). Laboratory insights  
1138 into the chemical and kinetic evolution of several organic molecules under  
1139 simulated Mars surface UV radiation conditions. *Icarus*, 242, 50-63.

1140 Rafkin, S. C., Pla-Garcia, J. et al. (2016). The meteorology of Gale Crater as  
1141 determined from Rover Environmental Monitoring Station observations and  
1142 numerical modeling. Part II: Interpretation. *Icarus*, 280, 114-138.

1143 Rafkin, S.C.R., (2009). A positive radiative-dynamic feedback mechanism for  
1144 the main- tenance and growth of Martian dust storms. *J. Geophys. Res.* 114,  
1145 E01009.

1146 Rafkin, S.C.R., Sta. Maria, M.R.V., Michaels, T.I., (2002). Simulation of the  
1147 atmospheric thermal circulation of a martian volcano using a mesoscale numerical  
1148 model. *Nature* 419, 697–699.

1149 Rafkin, S.C.R., Haberle, R.M., Michaels, T.I., (2001). The Mars Regional  
1150 Atmospheric Modeling System (MRAMS): Model description and selected  
1151 simulations. *Icarus* 151, 228–256.

1152 Schuerger, A. C., Moores, J. E., Clausen, C. A., Barlow, N. G., & Britt, D. T.  
1153 (2012). Methane from UV-irradiated carbonaceous chondrites under simulated  
1154 Martian conditions. *Journal of Geophysical Research: Planets*, 117(E8).

1155 Stevens, A. H., Patel, M. R., & Lewis, S. R. (2017). Modelled isotopic  
1156 fractionation and transient diffusive release of methane from potential subsurface  
1157 sources on Mars. *Icarus*, 281, 240-247.

1158 Steyn, D. G., De Wekker, S. F., Kossmann, M., & Martilli, A. (2013). Boundary  
1159 layers and air quality in mountainous terrain. In *Mountain Weather Research and*  
1160 *Forecasting* (pp. 261-289). Springer Netherlands.

1161 Sullivan, W., (1969). Two gases associated with life found on Mars near polar  
1162 cap. *New York Times* August 8, 1

1163 Vasavada, A. R., Piqueux, S., Lewis, K. W., Lemmon, M. T., & Smith, M. D.  
1164 (2017). Thermophysical properties along Curiosity's traverse in Gale crater, Mars,  
1165 derived from the REMS ground temperature sensor. *Icarus*, 284, 372-386.

1166 Villanueva, G. L. et al. (2013). A sensitive search for organics (CH<sub>4</sub>, CH<sub>3</sub>OH,  
1167 H<sub>2</sub>CO, C<sub>2</sub>H<sub>6</sub>, C<sub>2</sub>H<sub>2</sub>, C<sub>2</sub>H<sub>4</sub>), hydroperoxyl (HO<sub>2</sub>), nitrogen compounds (N<sub>2</sub>O,  
1168 NH<sub>3</sub>, HCN) and chlorine species (HCl, CH<sub>3</sub>Cl) on Mars using ground-based high-  
1169 resolution infrared spectroscopy. *Icarus*, 223(1), 11-27.

1170           Viscardy, S., Daerden, F., & Neary, L. (2016). Formation of layers of methane  
1171 in the atmosphere of Mars after surface release. *Geophysical Research Letters*,  
1172 43(5), 1868-1875.

1173           Webster et al. (2017). Mars Methane at Gale Crater Shows Strong Seasonal  
1174 Cycle: Updated Results from TLS-SAM on Curiosity. In AGU Fall Meeting 2017,  
1175 P33F-07.

1176           Webster, C. R. et al. (2015). Mars methane detection and variability at Gale  
1177 crater. *Science*, 347(6220), 415-417.

1178           Webster, C. R., Mahaffy, P. R., Atreya, S. K., Flesch, G. J., & Farley, K. A. (2013).  
1179 Low upper limit to methane abundance on Mars. *Science*, 1242902.

1180           Webster, C. R., & Mahaffy, P. R. (2011). Determining the local abundance of  
1181 Martian methane and its'  $^{13}\text{C}/^{12}\text{C}$  and  $\text{D}/\text{H}$  isotopic ratios for comparison with  
1182 related gas and soil analysis on the 2011 Mars Science Laboratory (MSL) mission.  
1183 *Planetary and Space Science*, 59(2), 271-283.

1184           Whiteman, C.D., Zhong, S., Shaw, W.J., Hubbe, J.M., Bian, X. and Mittelstadt, J.,  
1185 2001. Cold pools in the Columbia Basin. *Weather and Forecasting*, 16(4), pp.432-  
1186 447.

1187           Zahnle, K. (2015). Play it again, SAM. *Science*, 347(6220), 370-371.

1188           Zahnle, K., Freedman, R. S., & Catling, D. C. (2011). Is there methane on  
1189 Mars?. *Icarus*, 212(2), 493-503.